CMS-PPS-17-001
TOTEM 2018-001

Observation of proton-tagged, central (semi)exclusive production of high-mass lepton pairs in pp collisions at 13 TeV with the CMS–TOTEM precision proton spectrometer

The CMS and TOTEM Collaborations*

Abstract

The process $pp \rightarrow p\ell^+\ell^-p^{(*)}$, with $\ell^+\ell^-$ a muon or an electron pair produced at midrapidity with mass larger than 110 GeV, has been observed for the first time at the LHC in pp collisions at $\sqrt{s} = 13$ TeV. One of the two scattered protons is measured in the CMS–TOTEM precision proton spectrometer (CT–PPS), which operated for the first time in 2016. The second proton either remains intact or is excited and then dissociates into a low-mass state p^*, which is undetected. The measurement is based on an integrated luminosity of $9.4\,\mathrm{fb}^{-1}$ collected during standard, high-luminosity LHC operation. A total of 12 $\mu^+\mu^-$ and 8 e^+e^- pairs with $m(\ell^+\ell^-) > 110$ GeV, and matching forward proton kinematics, are observed, with expected backgrounds of $1.49 \pm 0.07\,(\text{stat}) \pm 0.53\,(\text{syst})$ and $2.36 \pm 0.09\,(\text{stat}) \pm 0.47\,(\text{syst})$, respectively. This corresponds to an excess of more than five standard deviations over the expected background. The present result constitutes the first observation of proton-tagged $\gamma\gamma$ collisions at the electroweak scale. This measurement also demonstrates that CT–PPS performs according to the design specifications.

*See Appendices A and B for the lists of collaboration members

arXiv:1803.04496v2 [hep-ex] 11 Aug 2018

1 Introduction

Proton–proton collisions at the LHC provide for the first time the conditions to study the production of particles with masses at the electroweak scale via photon–photon fusion [1, 2]. Although the production of high-mass systems in photon–photon collisions has been observed by the CMS and ATLAS experiments [3–5], no such measurement exists so far with the simultaneous detection of the scattered protons. This paper reports the measurement of the process $pp \to p\ell^+\ell^- p^{(*)}$ in pp collisions at $\sqrt{s} = 13\,TeV$, where a pair of leptons (ℓ = e, μ) with mass $m(\ell^+\ell^-) > 110\,GeV$ is reconstructed in the central CMS apparatus, one of the protons is detected in the CMS–TOTEM precision proton spectrometer (CT–PPS), and the second proton either remains intact or is excited and then dissociates into a low-mass state, indicated by the symbol p^*, and escapes undetected. Such a final state receives contributions from exclusive, $pp \to p\ell^+\ell^- p$, and semiexclusive, $pp \to p\ell^+\ell^- p^*$, processes (Fig. 1 left, and center). Central exclusive dilepton production is interesting because deviations from the theoretically well-known cross section may be an indication of new physics [6–8], whereas central semiexclusive processes constitute a background to the exclusive reaction when the final-state protons are not measured.

(Semi)exclusive dilepton production has been previously studied at the Fermilab Tevatron and at the CERN LHC, but at lower masses and never with a proton tag [9–14]. In this paper, forward protons are reconstructed in CT–PPS, a near-beam magnetic spectrometer that uses the LHC magnets between the CMS interaction point (IP) and detectors in the TOTEM area about 210 m away on both sides of the IP [15]. Protons that have lost a small fraction of their momentum are bent out of the beam envelope, and their trajectories are measured.

Central dilepton production is dominated by the diagrams shown in Fig. 1, in which both protons radiate quasi-real photons that interact and produce the two leptons in a t-channel process. The left and center diagrams result in at least one intact final-state proton, and are considered as signal in this analysis. The CT–PPS acceptance for detecting both protons in "exclusive" $pp \to p\ell^+\ell^- p$ events (the left diagram) starts only above $m(\ell^+\ell^-) \approx 400\,GeV$, where the standard model cross section is small. By selecting events with only a single tagged proton, the sample contains a mixture of lower mass exclusive and single-dissociation ($pp \to p\ell^+\ell^- p^*$, "semiexclusive") processes with higher cross sections. The right diagram of Fig. 1 is considered background, and contributes if a proton from the diffractive dissociation is detected, or if a particle detected in CT–PPS from another interaction in the same bunch crossing (pileup), or from beam-induced background is wrongly associated with the dilepton system. A pair of leptons from a Drell–Yan process can also mimic a signal event if detected in combination with a pileup proton.
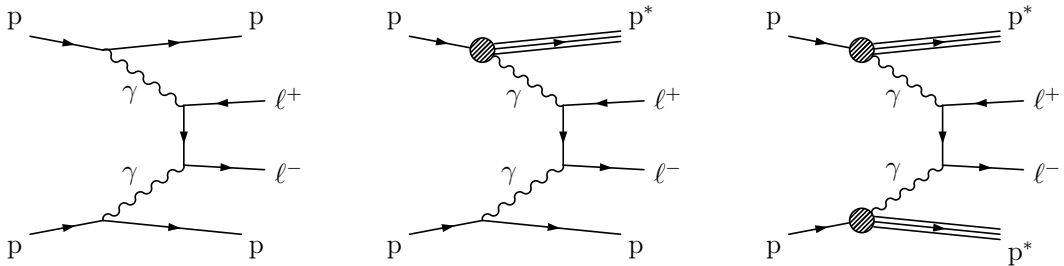

Figure 1: Production of lepton pairs by $\gamma\gamma$ fusion. The exclusive (left), single proton dissociation or semiexclusive (middle), and double proton dissociation (right) topologies are shown. The left and middle processes result in at least one intact final-state proton, and are considered signal in this analysis. The rightmost diagram is considered to be a background process.

In central (semi)exclusive events, the kinematics of the dilepton system can be used to determine the momentum of the proton, and hence its fractional momentum loss ξ. Comparison of this indirect measurement of ξ with the direct one obtained with CT–PPS can be used to suppress backgrounds, as well as to provide proof of the correct functioning of the spectrometer.

The CT–PPS detector [15, 16] operated for the first time in 2016 and collected a total integrated luminosity of $\sim$15 fb^{-1} in standard, high-luminosity runs of the LHC. The average number of pileup interactions per bunch crossing during 2016 was 27. For the present analysis, a sample of 9.4 fb^{-1} is used; the remaining (unused) data set was taken after September 2016, when the LHC collided protons with a different crossing angle.

The paper is organized as follows. Section 2 describes the experimental setup, and Sections 3–4 the procedures to derive the alignment and the LHC optics parameters from the data. Section 5 documents the samples of data and simulated events used in the analysis, while Sections 6 and 7 explain the event selection criteria, and the methods applied to estimate the backgrounds, respectively. Finally, the analysis and the results are presented in Section 8, followed by a summary in Section 9.

2 Experimental setup

The central feature of the CMS apparatus is a superconducting solenoid of 6 m internal diameter, providing a magnetic field of 3.8 T. Within the solenoid volume are a silicon pixel and strip tracker with coverage in pseudorapidity up to $|\eta| = 2.5$, a lead tungstate crystal electromagnetic calorimeter, and a brass and scintillator hadron calorimeter, each composed of a barrel and two endcap sections. Forward calorimeters extend the coverage provided by the barrel and endcap detectors up to $|\eta| = 5.2$. Muons are measured in gas-ionization detectors embedded in the steel flux-return yoke outside the solenoid. A more detailed description of the CMS detector, together with a definition of the coordinate system used and the relevant kinematic variables, can be found in Ref. [17].

The CT–PPS detector measures protons scattered at small angles and carrying between about 84 to 97% of the incoming beam momentum. These protons remain inside the beam pipe and their trajectory is measured by a system of position-sensitive detectors at a distance of about 210 m from the IP, on both sides of CMS. These tracking detectors are complemented by timing counters to measure the proton arrival time. The detector planes are inserted horizontally into the beam pipe by means of "Roman Pots" (RPs), i.e. movable near-beam devices that allow the detectors to be brought very close (down to a few mm) to the beam without affecting the vacuum, beam stability, or other aspects of the accelerator operation.

The layout of the beam line from the IP to the 210 m region on one of the two sides of CMS is shown in Fig. 2. The two sides are referred to as "arms" in the following. The arms to the left (positive z direction) and to the right of CMS when looking from the center of the LHC correspond to LHC sectors 45 and 56 on the two sides of interaction point 5 where CMS is located, respectively. In each arm there are two tracking units, referred to as "210 near" (210N) and "210 far" (210F), which are located at 203.8 m and 212.6 m from the IP, respectively. In 2016, the tracking RPs were each instrumented with 10 planes of edgeless silicon strip sensors, providing a spatial resolution of about 12 μm. Five of these planes are oriented with the silicon strips at a $+45°$ angle with respect to the bottom of the RP, while the other five have the strips at a $-45°$ angle. In total each RP silicon detector plane contains 512 individual strips, with a pitch of 66 μm. A schematic diagram of the silicon strip sensors, indicating their orientation relative to the LHC beam, is shown in Fig. 3

The hit efficiency per plane is estimated to be >97% before the effect of radiation damage to the sensors. The signal from the silicon detectors is contained within one 25 ns bunch crossing of the LHC. The data are read out using a digital VFAT chip [18], and recorded through the standard CMS data acquisition system. The pots as well as the sensors have been extensively used by the TOTEM experiment and are described in Refs. [16, 19]. The TOTEM silicon strip sensors were not designed to sustain exposure to the high radiation doses of the standard high-luminosity LHC fills. As expected, a first set of such planes suffered severe radiation damage after about $10\,\text{fb}^{-1}$, and was replaced by a set of spares. In order to operate at high instantaneous luminosity, the RPs have been equipped with special ferrite shielding, so as to reduce their electromagnetic impedance, and hence limit their impact on the LHC beams. The timing detectors are housed in low-impedance, cylindrical RPs specially built for CT–PPS, located at 215.7 m from the IP. They were equipped with diamond detectors for the last part of the run to complement the tracking silicon strip detectors. They are not used for the analysis discussed here. In its final configuration, CT–PPS will use 3D silicon pixel sensors for tracking and diamond sensors for timing.
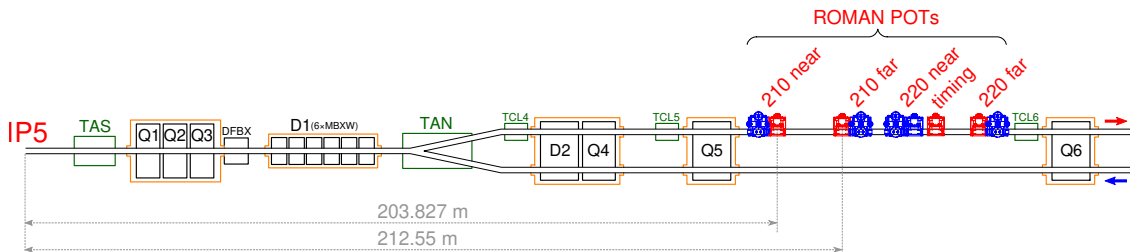

Figure 2: Schematic layout (not to scale) of the beam line as seen from above between the interaction point (IP5) and the region where the RPs are located in LHC sector 56. Dipole magnets (D1, D2) of single- (MBXW) and twin-aperture, quadrupoles (Q1–Q6), collimators (TCL4–TCL6), absorbers (TAS, TAN), and quadrupole feedboxes (DFBX) are shown. The 210 near and 210 far units are indicated, along with the timing RPs not used here. The 220 near and 220 far units (not used here) are also shown. The RPs indicated in red are the horizontal CT–PPS ones; those in blue are part of the TOTEM experiment. The red (blue) arrow indicates the outgoing (incoming) beam. In the CMS coordinate system, the z axis points to the left. The arm in the opposite LHC sector 45 (not shown) is symmetric with respect to the IP.

The data analyzed for this paper were collected with the RPs at a distance of about $15\,\sigma$ from the beam, where σ is the standard deviation of the spatial distribution of the beam in the transverse direction pointing to the RP; the values of σ range from 0.245 mm for the 210N RP to 0.14 mm for the timing RP.

3 Alignment of the CT–PPS tracking detectors

Alignment of CT–PPS is required in order to determine the position of the sensors with respect to each other inside a RP, the relative position of the RPs, and the overall position of the spectrometer with respect to the beam. An overview of the procedure is given here; more details are available in Ref. [20].

The alignment procedure consists of two conceptually distinct parts:

- Alignment in a special, low-luminosity calibration fill ("alignment fill"), where RPs are inserted very close to the beam (about $5\,\sigma$).
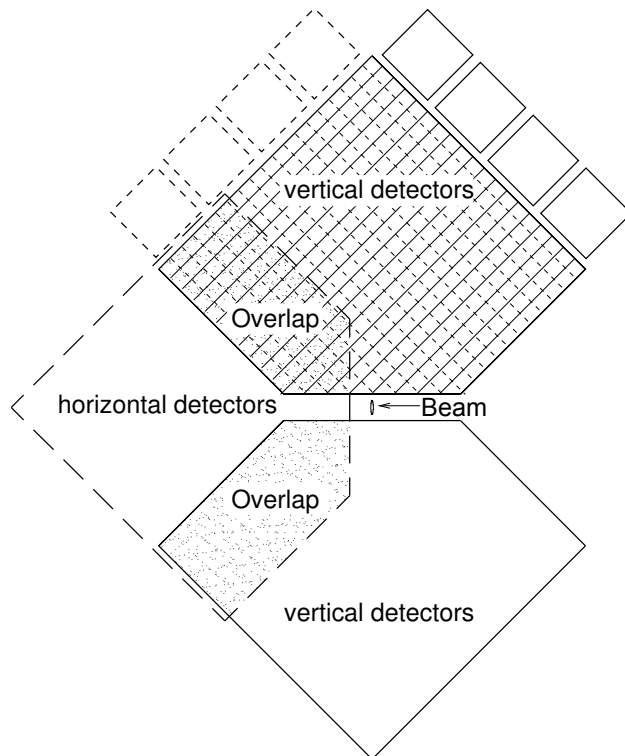- Transfer of the alignment information to the standard, high-luminosity physics fills.

Figure 3: Schematic layout of the silicon strip detectors in one RP station. Both the horizontal RP and the vertical RPs, which are used only for special low-luminosity calibration fills, are shown. In the top RP, the silicon strips oriented at $+45°$ and $-45°$ angles are indicated by the diagonal lines. Tracks in the overlap region, indicated by the shaded area, are used to perform a relative alignment of the RPs in the calibration fills.

3.1 Alignment fill

The first step is the beam-based alignment, the purpose of which is to establish the position of the RPs with respect to the LHC collimators and the beam. It takes place only once per LHC optics setting. In this procedure, the TOTEM vertical RPs [19] (cf. Fig. 3) are used together with the horizontal CT–PPS RPs. The beam is first scraped with the collimators so that it develops a sharp edge. Then each RP is moved in small (approximately $10\,\mu$m) steps until it is in contact with the edge of the beam, which generates a rapid increase in the rate observed in the beam-loss monitors close to CT–PPS. At this point, each RP is at the same distance (in units of σ) as the collimator, i.e. the RP is at the edge of the shadow cast by the collimator. The necessity to get very close to the beam stems from the need of having the TOTEM vertical and the CT–PPS RPs overlap. Data are then taken in this configuration, with the horizontal and vertical RPs at 8 and $5\,\sigma$, respectively.

The second step consists of determining the relative position of all the sensors in each arm using the data from the alignment fill. This is achieved by minimizing the residuals between hit positions and fitted tracks. The track reconstruction is described in Section 4.2. The position (shift perpendicular to the beam) and rotation (about the beam axis) of each sensor are thereby determined. While no event selection is necessary (since the method assumes that the tracks are linear, which is the case as there are no magnets at the RP location), the most valuable events are those with tracks reconstructed when the RP detectors overlap, which allow the relative alignment of the RPs to be determined. The method is applied to several data subsamples in order to verify the stability of the results.

Finally, the alignment of CT–PPS with respect to the beam is performed, again with data from the dedicated fill. A sample of several thousand elastic scattering events, pp → pp, is used for that purpose. The LHC optics causes the elastic hit distribution in any vertical RP to have an elliptical shape centered on the beam position. This symmetry is exploited to determine the position of the RP with respect to the beam.

The uncertainties in the results of the procedure just discussed are 5 mrad for rotations, 50 μm for horizontal shifts, and 75 μm for vertical shifts.

3.2 Physics fills

Since the RPs move, and the beam position can change, the position of CT–PPS with respect to the beam needs to be redetermined for each fill. The physics fills are characterized by high intensity with only the horizontal RPs inserted at much larger distances (about 15 σ) from the beam than in the alignment fill, and therefore a different procedure is employed.

The horizontal alignment is based on the assumption that the scattered protons from a pp collision at the IP have the same kinematic distributions in all fills. Given the stability of the LHC conditions (RP positions, collimator setting, magnet currents, and beam orbit), this leads to the spatial distributions of the track impact points observed in the RPs (Section 4.2). The alignment is then achieved by matching these distributions from a physics fill to those from the alignment fill. An example of this procedure is shown in Fig. 4. For this method to work, it is important to suppress the background due to secondary interactions taking place between the IP and the RPs. To this end, the correlation between the coordinates of the horizontal hit positions in the near and far RPs is used. The total uncertainty of the horizontal alignment is about 150 μm.
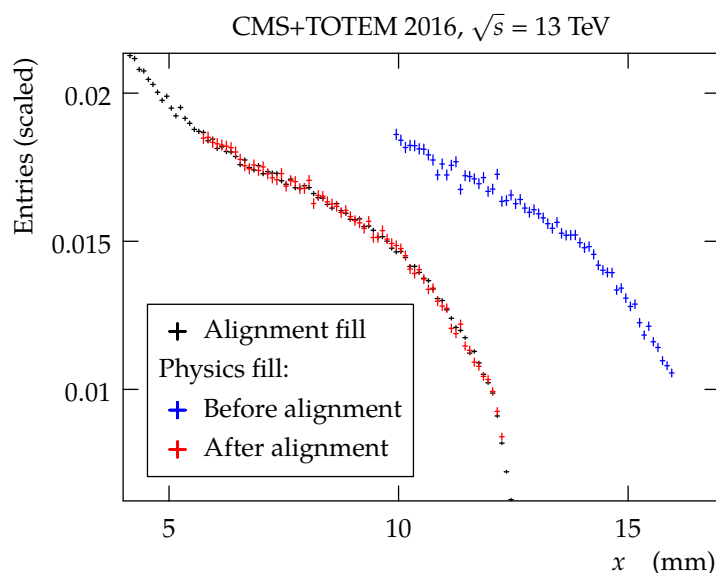

Figure 4: Distribution of the track impact points as a function of the horizontal coordinate for the alignment fill (black points), a physics fill before alignment (blue points), and after alignment (red points). The beam center is at $x = 0$ for the black and red points; the x axis origin is undefined for the blue points. In the alignment procedure the overall normalization of the histogram is irrelevant; the histograms from different fills are therefore rescaled to compare their shapes.

The beam vertical position with respect to the sensors is determined by fitting a straight line

to the y coordinate of the maximum of the track impact point distribution as a function of x (horizontal beam position). The fitted function is then extrapolated to $x = 0$. This procedure can be applied since, unlike for the horizontal case, the maximum of the vertical distribution is within the acceptance of the horizontal RPs. Here again, the resulting uncertainty is of the order of $150\,\mu$m.

4 Proton reconstruction

4.1 The LHC beam optics

The reconstruction of the scattered proton momentum from the tracks measured in the RPs requires precise knowledge of the magnetic fields traversed by the proton from the IP to the RPs [21]. This is normally parametrized in terms of the "beam optics", in which the elements of the beam line are treated as optical lenses. The proton trajectory is described by means of transport matrices, which transform the kinematics of protons scattered at the IP to the kinematics measured at the RP position. The trajectory of protons produced at the IP (denoted by the superscript '*') with transverse vertex position (x^*, y^*) and horizontal and vertical components of scattering angle (Θ_x^*, Θ_y^*) is described approximately by:

$$\mathbf{d}(s) = T(s, \xi)\mathbf{d}^*, \tag{1}$$

where s indicates the distance from the IP along the nominal beam orbit, and $\mathbf{d} = (x, \Theta_x, y, \Theta_y, \xi)$, with $\xi = \Delta p / p$, and p and Δp the nominal beam momentum and the proton longitudinal momentum loss, respectively. The symbol $T(s, \xi)$ denotes the single-pass transport matrix, whose elements are the optical functions. The leading term in the horizontal plane is:

$$x = D_x(\xi)\xi, \tag{2}$$

where the dispersion D_x has a mild dependence on ξ. In the vertical plane, the leading term reads:

$$y = L_y(\xi)\Theta_y^*, \tag{3}$$

where $L_y(\xi)$ is the vertical effective length. The ξ dependence of L_y is shown in Fig. 5. At any location s in the RP region there is a value of ξ, ξ_0, where L_y vanishes and hence the values of y concentrate around zero. Consequently, the distribution of the track impact points exhibits a 'pinch' at $x_0 \approx D_x \xi_0$, cf. Fig. 6. The horizontal dispersion D_x is then estimated as:

$$D_x \approx \frac{x_0}{\xi_0}. \tag{4}$$

The subleading terms neglected in this approximation are treated as systematic uncertainties.

An independent estimate of the difference of the dispersions in the two LHC beams, ΔD_x, is obtained by varying ΔD_x to find the best match between the ξ distributions reconstructed from the two arms. This estimate agrees with the one discussed above within the uncertainties.

These two horizontal dispersion measurements and the beam position values constrain the LHC optics between the IP and the RPs, including the nonlinearities of the proton transport matrices and their dependence on ξ. The optical functions are extracted with the methods originally developed for the analysis of elastic scattering data [23].
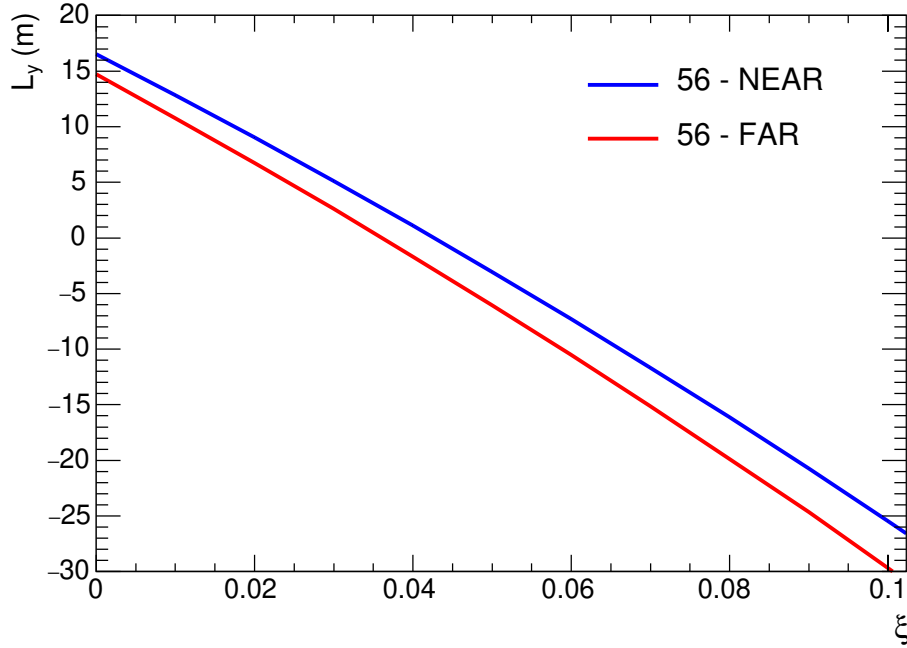
Figure 5: Vertical effective length L_y (in meters) as a function of the proton relative momentum loss ξ at two (near and far) RPs calculated with the beam line optics simulation program MAD-X [22].
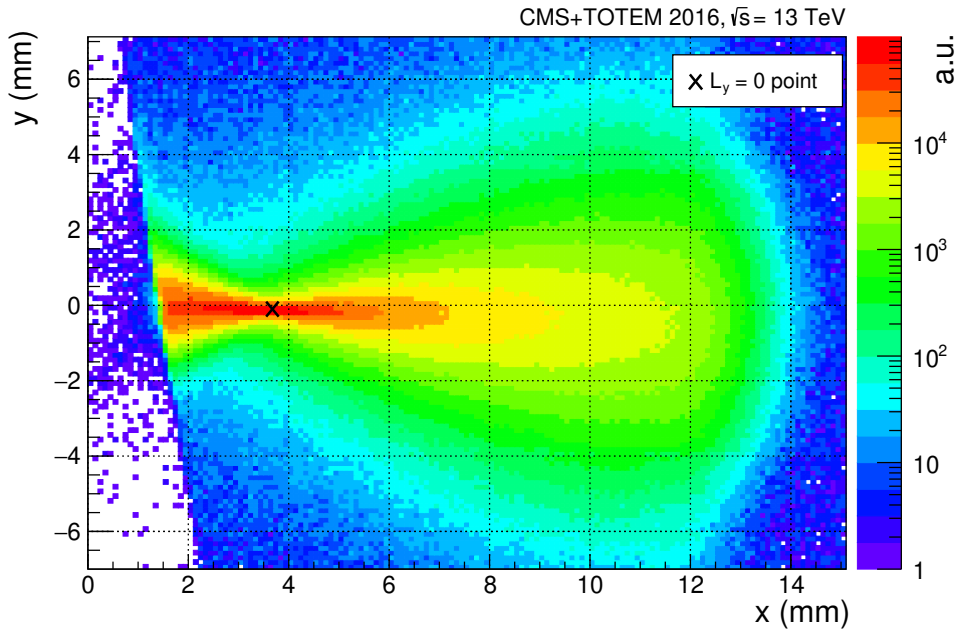

Figure 6: Distribution of the track impact points measured in RP 210F, in sector 45, for the alignment fill. The point where $L_y = 0$ is shown with a cross. The beam center is at $x = y = 0$. The edge of the distribution is slanted because the RP shown has a rotation of $8°$ with respect to the vertical.

4.2 Proton track reconstruction

Since there is no significant magnetic field in the region of the CT–PPS RPs, the trajectory of particles passing through the silicon strip detectors is a straight line. In each RP (RP hereinafter

refers to the particle detector contained in the pot), track reconstruction therefore starts with a search for linear patterns along z among the hits detected in the 10 planes, as described in Chapter 3 of Ref. [24]. The search is performed independently in each of the two strip orientations (with angles of $+45°$ and $-45°$ with respect to the bottom of the RP); hits in at least 3 out of 5 planes are required. If only one pattern is found in both orientations, the patterns can be uniquely associated and a track fitted, yielding a "track impact point" evaluated at the center of the RP along z. Figure 7 shows a typical distribution of the track impact points in the (x, y) plane for a RP at $15\,\sigma$ from the beam. When there is more than one pattern in any strip orientation, a unique association is not possible and no track is reconstructed. The inefficiency due to multiple tracks depends on the pileup, and ranges between 15 and 40% in the 2016 data used in this analysis. This multiple tracks inefficiency and the ξ- and time-dependent effects of radiation damage to the sensors described in Section 2 are the dominant sources of inefficiency. Other reconstruction effects, such as those due to showers within the detector material, are estimated to contribute $\approx$3% to the efficiency for finding proton tracks.
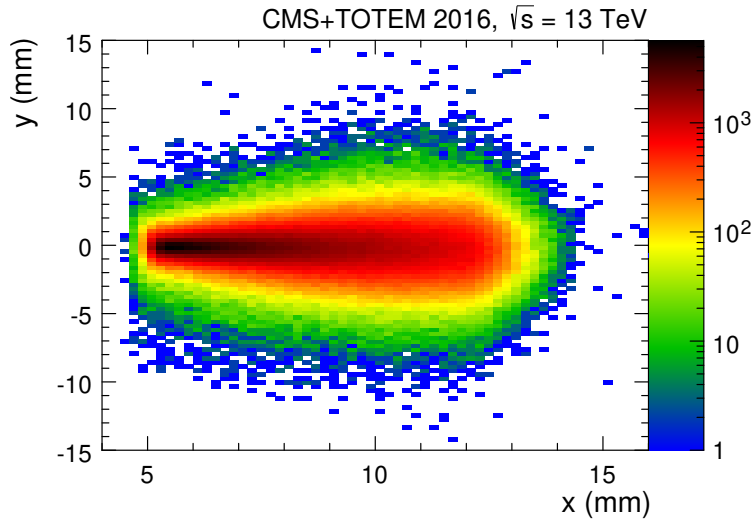

Figure 7: Example of track impact point distribution (in the x, y plane) measured in RP 210F, sector 45, at $15\,\sigma$ from the beam in the x direction. The beam center is at $x = y = 0$. The track selection includes a matching requirement with RP 210N, which suppresses noise and beam backgrounds, but slightly reduces the acceptance for low values of the position x, given the different acceptance of the near and far RPs.

4.3 Determination of ξ

The fractional momentum loss of a proton, ξ, can be determined from the track impact point in a single RP. This is advantageous in regions where the other RP of the sector does not have sufficient acceptance or is inefficient. In practice, ξ is reconstructed by inverting Eq. (2). This method ignores subleading terms in the proton transport (notably the one proportional to the horizontal scattering angle); their effect is included in the systematic uncertainties.

The main uncertainties are:

- dispersion calibration: relative uncertainty in D_x of about 5.5%;
- horizontal alignment: approximately 150 μm;
- neglected terms in Eq. (2).

For values of $\xi \gtrsim 0.04$, the leading uncertainty comes from the dispersion, and from the ne-

glected terms related to Θ_x^* in Eq. (2).

Having reconstructed ξ, Eq. (3) can then be used to determine the vertical scattering angle from the curves presented in Fig. 5. The scattering angle can, in turn, be related to the vertical component of the proton transverse momentum.

5   Data sets and Monte Carlo samples

The CT–PPS data analyzed here were collected during the period May–September 2016; they correspond to an integrated luminosity of $9.4\,\mathrm{fb}^{-1}$. In the same period, CMS collected a total of $15.6\,\mathrm{fb}^{-1}$. For the present data, the beam amplitude function β^* at the IP was 0.4 m and the crossing angle α_x of the beams was $370\,\mu$rad. After about a month, the silicon strip detectors suffered heavy radiation damage. After new silicon strip detectors were installed in September, the LHC implemented a smaller crossing angle for collisions at the CMS IP, which resulted in different optics parameters and therefore changed the CT–PPS acceptance. These later data are therefore not used in the present analysis.

Simulated signal samples of exclusive (pp $\to$ p$\ell^+\ell^-$p) and single proton dissociative (pp $\to$ p$\ell^+\ell^-$p*) events proceeding via photon fusion $\gamma\gamma \to \ell^+\ell^-$ are generated with the LPAIR code [25, 26] (version 4.2). LPAIR is also used to produce $\gamma\gamma \to \ell^+\ell^-$ samples with both protons exciting and dissociating, that is pp $\to$ p$^*\ell^+\ell^-$p*. These three topologies are illustrated in Fig. 1. The central detector information is passed through the standard GEANT4 [27] simulation of the CMS detector and reconstructed in the same way as the collision data. Conversely, only generator-level forward proton information is used, which is sufficient for the present analysis.

Background from the Drell–Yan process, pp $\to \gamma^*/\mathrm{Z}^* \to \ell^+\ell^- + X$, is simulated with MADGRAPH5_aMC@NLO [28, 29], interfaced with the PYTHIA 8.212 [30] event generator using the CUETP8M1 tune [31] for parton showering, underlying event, and hadronization. The events are generated at leading order, and normalized to the next-to-next-to-leading order cross section prediction [32].

6   Event selection

6.1   Central variables

Events were selected online [33] by requiring the presence of at least two muon (electron) candidates of any charge, each with transverse momentum $p_\mathrm{T} > 38\,(33)\,\mathrm{GeV}$. No requirement on forward protons was imposed online.

Offline, the tracks of the two highest-p_T lepton candidates of the same flavor in the event are fitted to a common vertex. The vertex position from the fit is required to be consistent with that of a collision ($|z| < 15\,\mathrm{cm}$), with a $\chi^2 < 10$ (probability greater than 0.16% for 1 degree of freedom). The lepton candidates are further required to have $p_\mathrm{T} > 50\,\mathrm{GeV}$, and to pass the standard CMS quality criteria [34, 35]. In the final stage of the analysis only leptons with opposite charge are retained. No explicit isolation is required for the leptons; however, non-prompt leptons (i.e. from heavy and light hadron decays in flight) are heavily suppressed by the applied track multiplicity criteria described below.

In order to select a sample enriched in $\gamma\gamma \to \ell^+\ell^-$ events, a procedure similar to that of the Tevatron and Run 1 LHC analyses [3–5, 9–11, 13, 36] is used. The event is accepted if no additional tracks are found in the region within the veto distance around the dilepton vertex. No

explicit requirement is made on the p_T or on the quality of these extra tracks. In addition, the dilepton acoplanarity ($a = 1 - |\Delta\phi(\ell^+\ell^-)|/\pi$) is required to be consistent with the two leptons being back-to-back in azimuth ϕ. The dilepton acoplanarity versus the distance between the closest extra track and the dilepton vertex is shown in Fig. 8 for muons (left) and electrons (right), for the simulated signal (blue and green dots) and double-dissociation and Drell–Yan backgrounds (red and yellow dots). Based on these distributions, an extra-track veto region distance of at least 0.5 mm around the vertex is required, along with $a < 0.009$ for the muons and $a < 0.006$ for the electrons. The acoplanarity requirements are chosen such that the signal to background ratio predicted by the simulation is above unity before any matching of the leptons with RP tracks. The size of the extra-track veto region is smaller than suggested by the simulation, reflecting the fact that the distribution of primary vertices in z is narrower in the data than in the simulation. Because of the high pileup rate, the selection is based on information from reconstructed tracks alone, without using information from the calorimeters. This results in an efficiency of $> 95\%$ for the highest values of pileup and pileup density observed in the 2016 data set used for the measurement.
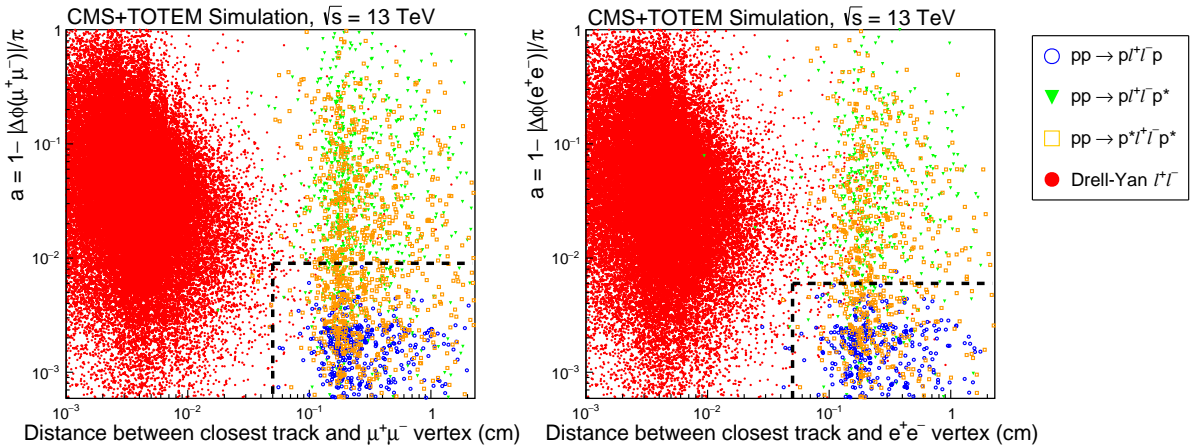
Figure 8: Dimuon (left) and dielectron (right) acoplanarity versus the distance between the closest extra track and the dilepton vertex for simulated signal and backgrounds. The points represent the Drell–Yan (red), exclusive $\gamma\gamma \to \ell^+\ell^-$ (blue), single-dissociative $\gamma\gamma \to \ell^+\ell^-$ (green), and double-dissociative $\gamma\gamma \to \ell^+\ell^-$ (yellow) processes. The dashed lines indicate the region selected for the analysis. The number of points for each physics process does not reflect its cross section.

Finally, the invariant mass of the leptons is required to satisfy $m(\ell^+\ell^-) > 110$ GeV. This suppresses the region around the Z boson mass, which is expected to be dominated by Drell–Yan production.

Figure 9 shows the distributions of the dimuon and dielectron invariant mass and rapidity y, after all the central detector requirements just described are applied. The Monte Carlo (MC) predictions are normalized to the total integrated luminosity. In addition, for the LPAIR predictions, rapidity gap survival probabilities of 0.89, 0.76, and 0.13 are applied to the exclusive, the single dissociative, and the double dissociative processes, respectively. The rapidity gap survival probability quantifies the fraction of events in which no extra soft interactions occur between the colliding protons. These soft interactions produce extra final-state particles, and thereby suppress the visible (semi)exclusive cross section. The values used are calculated from modified photon parton distribution functions in the proton that are compatible with Run 1 LHC measurements. In the case of the proton dissociation processes, these values represent a mix of the incoherent and QCD evolution terms calculated in Ref. [37]. This choice of ra-

pidity gap survival probabilities leads to a fair description of the data for y around zero, but overestimates the results at more forward/backward rapidities, as is clear from the bottom panels of Fig. 9. A y dependence of the rapidity gap survival probability is expected in several models [38, 39].
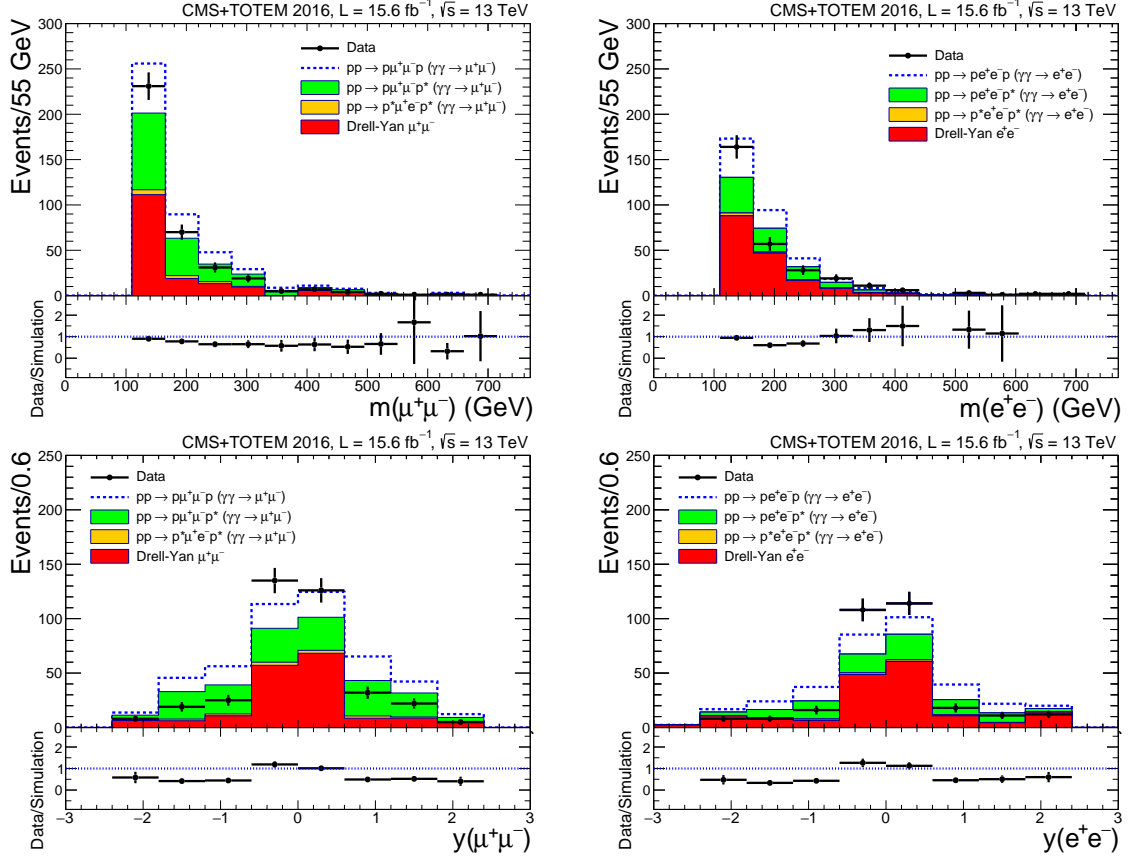

Figure 9: Dimuon (left) and dielectron (right) invariant mass (top) and rapidity (bottom), after all central-detector criteria are applied, in pp collisions at 13 TeV. Points with error bars indicate the measured data (with statistical uncertainties only), and the stacked histograms show the different simulated contributions for signal and backgrounds (with statistical uncertainty of similar size as the data). The lower panel in each plot shows the ratio of the data to the sum of all signal and background predictions.

6.2 Matching central and proton variables

Events with at least one well-reconstructed proton track in CT–PPS are retained for further analysis. For each event, the value of the fractional momentum loss of the scattered proton is estimated from the leptons as:

$$\xi(\ell^+\ell^-) = \frac{1}{\sqrt{s}}\left[p_\mathrm{T}(\ell^+)e^{\pm\eta(\ell^+)} + p_\mathrm{T}(\ell^-)e^{\pm\eta(\ell^-)}\right],\qquad(5)$$

where the two solutions for $\pm\eta$ correspond to the protons moving in the $\pm z$ direction.

The formula is exact for exclusive events, but holds also for the single-dissociation case, as illustrated with LPAIR simulated events in Fig. 10; in this case only one of the two possible solutions will correspond to the direction of the intact proton. Studies with LPAIR indicate that a mass of the dissociating system larger than about 400 GeV is needed in order to produce a deviation

comparable to the expected $\xi(\ell^+\ell^-)$ resolution of about 3% (4%) for dimuons (dielectrons). The latter is obtained from simulation, with an additional smearing to account for residual data–simulation differences. The LPAIR simulation also indicates that the minimum mass of the dissociating system required to generate activity in the CMS tracker is about 50 GeV; the fraction of dissociative events above this threshold is of a few percent.
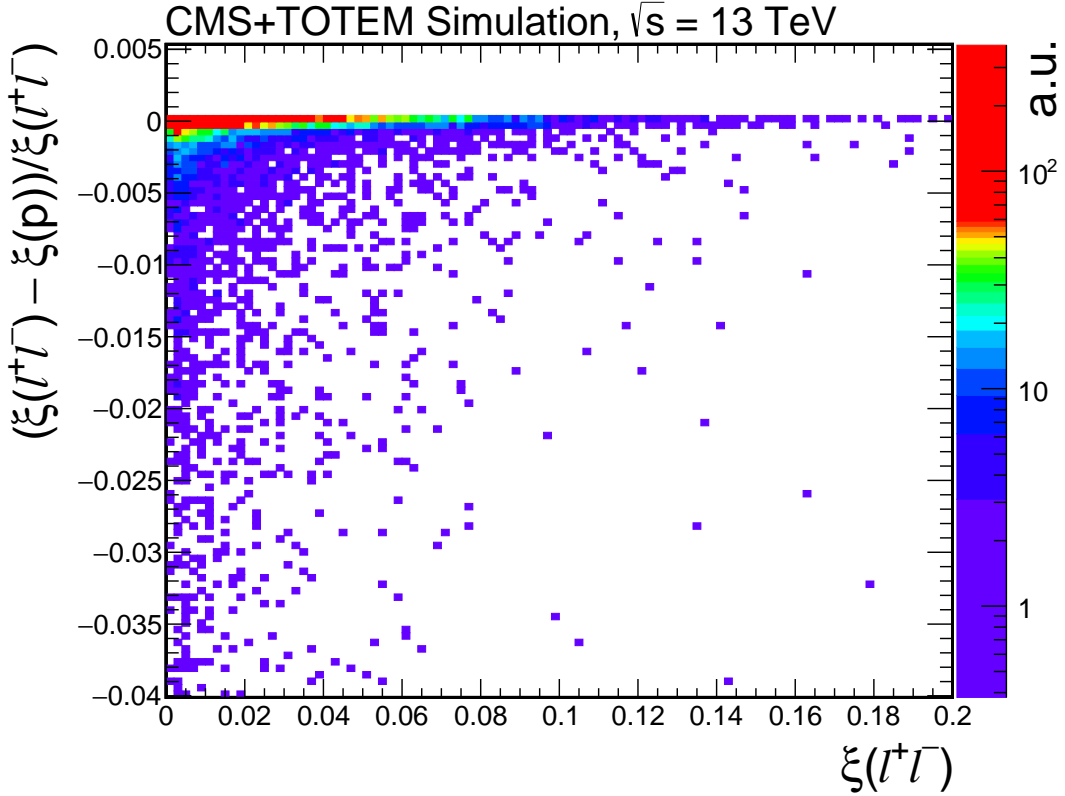

Figure 10: Generator-level relative difference $(\xi(\ell^+\ell^-) - \xi(\mathrm{p}))/(\xi(\ell^+\ell^-))$ vs. $\xi(\ell^+\ell^-)$ for simulated single dissociative $\gamma\gamma \to \ell^+\ell^-$ events. Of the two possible solutions for $\xi(\ell^+\ell^-)$, only the one corresponding to the side with the intact proton is shown.

To be considered as signal candidates, events are further required to have a value of $\xi(\ell^+\ell^-)$ within the CT–PPS coverage. The minimum value of ξ observed in an inclusive sample of dilepton-triggered events, with no selection to enhance $\gamma\gamma$ production, is used. Numerically this corresponds to:

- sector 45, RP 210N: $\xi > 0.033$,
- sector 45, RP 210F: $\xi > 0.024$,
- sector 56, RP 210N: $\xi > 0.042$,
- sector 56, RP 210F: $\xi > 0.032$.

The difference between the ξ coverage in the sectors 45 and 56 is due to the asymmetric beam optics.

Finally, the signal region is defined by requiring that $\xi(\ell^+\ell^-)$ and the corresponding value measured with CT–PPS, $\xi(\mathrm{RP})$, agree within 2σ of the combined uncertainty on $\xi(\ell^+\ell^-)$ and D_x.

7 Backgrounds

After all selection criteria discussed above, the backgrounds are expected to arise mainly from prompt $\ell^+\ell^-$ production combined with proton tracks from unrelated pileup interactions or beam backgrounds in the same bunch crossing. The largest background sources of prompt $\ell^+\ell^-$ production are the Drell–Yan process and $\gamma\gamma \to \ell^+\ell^-$ production in which both protons dissociate.

To estimate both the Drell–Yan and the double dissociative backgrounds, samples of RP tracks from $Z \to \mu^+\mu^-$ and $Z \to e^+e^-$ events in data are used (referred to as "Z control samples" in the following). For the double dissociative background estimate, LPAIR simulated events are also used, in conjunction with the RP tracks from the Z control samples. To avoid statistical correlations between the two estimates, only every second event from each sample is considered for the Drell–Yan estimate, and the remaining part for the double-dissociative background. In both cases, the background estimation is mostly based on data, and does not require detailed knowledge of the RP acceptance and detector efficiency. The procedure is described in the following.

- The extra track and acoplanarity selection criteria are not applied to estimate the Drell–Yan background. Instead, an invariant mass window of $80 < m(\ell^+\ell^-) < 110\,\text{GeV}$ is imposed, resulting in a high purity sample of Drell–Yan events. A subsample is then selected with a proton track matching the kinematics of the $\ell^+\ell^-$ pair. The Drell–Yan events in this subsample tend to be concentrated at midrapidity, which causes a distortion of the $\xi(\ell^+\ell^-)$ distribution. The distribution is therefore reweighted to match the shape predicted by the Drell–Yan simulation for events entering the signal region, with $m(\ell^+\ell^-) > 110\,\text{GeV}$. Finally, the simulated Drell–Yan sample is used to obtain the number of matching events expected to pass the track multiplicity, acoplanarity, and $m(\ell^+\ell^-)$ requirements, given the number observed in the Z boson control sample.

- In the case of the background from double dissociation dilepton production, simulated double dissociation LPAIR events are randomly mixed with the background-dominated sample of protons from the Z boson control sample. The protons from this sample are used for convenience, and any other sample of protons could have been used; the information from the central part of the event is not necessary for the present study.

  The MC events passing the central detector requirements are selected, and an exponential function is fitted to the corresponding $\xi(\ell^+\ell^-)$ distribution. Then a fast simulation is performed in which the fit is sampled, and the value of $\xi(\ell^+\ell^-)$ is randomly assigned to a proton from the Z boson sample.

  The background estimate is obtained from the number of events in the fast simulation that pass the proton selection (cf. Section 6.2) in addition to the central detector requirements, normalized to the number of MC events passing the central signal selection. The procedure just described forces all double dissociation events to have a background proton in CT–PPS. The background estimate thus needs to be scaled by the fraction of events passing the central selection that do not have a proton in CT–PPS. This is obtained from the data.

  For the simulation of the double dissociation process, the y-independent rapidity gap survival probability of 0.13 quoted above is used. If instead the y-dependent rapidity gap survival probability discussed in Section 6 were used, the dissociative background and total background estimates would decrease. The present estimate

Table 1: Estimated backgrounds from Drell–Yan and double-dissociation $\mu^+\mu^-$ production, within the acceptance of at least one of the RPs of a given arm, and in the subsample with proton kinematics matching within 2σ. The bottom row indicates the total background from the sum of Drell–Yan and double dissociation events.

Arm and background source	Full	2σ
Left Drell–Yan	6.14 ± 0.13	0.75 ± 0.05
Right Drell–Yan	5.22 ± 0.12	0.63 ± 0.04
Total Drell–Yan	11.36 ± 0.18	1.38 ± 0.06
Left double dissociation	0.57 ± 0.01	0.046 ± 0.003
Right double dissociation	0.60 ± 0.01	0.062 ± 0.004
Total double dissociation	1.17 ± 0.02	0.108 ± 0.005
Total background	12.52 ± 0.18	1.49 ± 0.07

Table 2: Estimated backgrounds from Drell–Yan and double-dissociation e^+e^- production, within the acceptance of at least one of the RPs of a given arm, and in the subsample with proton kinematics matching within 2σ. The bottom row indicates the total background from the sum of Drell–Yan and double dissociation events.

Arm and background source	Full	2σ
Left Drell–Yan	6.24 ± 0.13	1.07 ± 0.06
Right Drell–Yan	6.09 ± 0.14	1.23 ± 0.06
Total Drell–Yan	12.33 ± 0.19	2.30 ± 0.09
Left double dissociation	0.31 ± 0.01	0.035 ± 0.002
Right double dissociation	0.25 ± 0.01	0.032 ± 0.002
Total double dissociation	0.56 ± 0.01	0.067 ± 0.003
Total background	12.89 ± 0.19	2.36 ± 0.09

    is thus conservative.

- The dissociating system may contain a final-state proton that falls within the CT–PPS acceptance, even without overlap of an unrelated proton. However, the simulation indicates that the total number of such events within the acceptance is negligible.

The numbers of background events expected with tracks in either or both of the near and far RPs in each arm are shown in Tables 1–2. A total of 11.0 ± 0.2 (stat) dimuon events and 10.5 ± 0.2 (stat) dielectron ones are expected within the acceptance, but outside the 2σ matching window. Within the 2σ matching window, the total background prediction is 1.49 ± 0.07 (stat) dimuon events and 2.36 ± 0.09 (stat) dielectron events with a matching track in at least one RP, in both arms combined.

The systematic uncertainties in the Drell–Yan and double dissociation backgrounds are shown in Table 3 and are estimated as follows. A 5% contribution is assigned to reflect the statistical uncertainty of the control sample of protons from the Z boson mass region for the dimuon case, and a 4% contribution for the dielectron channel. In addition, the Drell–Yan background estimate is affected by uncertainties related to the reweighting of the $\xi(\ell^+\ell^-)$ distribution and the modeling of the track multiplicity distribution in the simulation. The former is obtained as the difference of the background estimates with and without reweighting, leading to a 25% (11%) relative uncertainty in the dimuon (dielectron) channel. The latter is estimated from the difference between data and simulation in the low-multiplicity region, with 1–5 additional tracks

Table 3: Sources of systematic uncertainties in the estimates of Drell–Yan and double-dissociation backgrounds in the dimuon and dielectron channels.

	$\mu^+\mu^-$		e^+e^-	
Sources of uncertainty	Drell–Yan	Double diss.	Drell–Yan	Double diss.
Statistics of Z sample	5%	5%	4%	4%
$\xi(\ell^+\ell^-)$ reweighting	25%	—	11%	—
Track multiplicity modeling	28%	—	14%	—
Survival probability	—	100%	—	100%
Luminosity	—	2.5%	—	2.5%

near the dilepton vertex, resulting in 28 and 14% relative uncertainties for the dimuon and dielectron channels, respectively. The double-dissociation process has never been measured directly, and therefore the background estimate for this process also includes a 100% relative uncertainty on the rapidity gap survival probability. Finally, the double-dissociation background includes a 2.5% integrated luminosity uncertainty [40] applied to the normalization of the simulated samples.

As a further check of the pileup background estimate, a set of pseudo-experiments is performed in which the measured values of $\xi(\ell^+\ell^-)$ within the CT–PPS acceptance are randomly coupled with $\xi(p)$ values from events without any offline selection imposed on the central variables. The dilepton system and the proton originate from different events and are thus uncorrelated. Such a procedure is repeated 10^4 times, and the average number of events in which $\xi(\ell^+\ell^-)$ and $\xi(p)$ match within 2σ is determined. The result is consistent with the background estimates of 1.49 ± 0.07 (stat) and 2.36 ± 0.09 (stat) events discussed above for the dimuon and dielectron channels, respectively.

8 Results

In the $\mu^+\mu^-$ channel, a total of 17 events are observed with $\xi(\mu^+\mu^-)$ within the CT–PPS acceptance, and at least one track detected in the relevant RPs. Five of those events have a mismatch of $\geq 2\sigma$ between the dimuon and the proton kinematics, compared to 11.0 ± 4.0 (stat+syst) such events expected from background; twelve events have a track in at least one of the two RPs matching $\xi(\mu^+\mu^-)$ within 2σ. The significance of observing 12 events over the background estimate of 1.49 ± 0.07 (stat) ± 0.53 (syst) is 4.3σ, estimated by performing pseudo-experiments according to a Poisson distribution, including the systematic uncertainties profiled as log-normal nuisance parameters.

The invariant masses and rapidities of the $\mu^+\mu^-$ candidate events are consistent with the expected single-arm acceptance, given the LHC optics and the position of the RPs. No events are observed with matching protons in both arms; the highest-mass event is at $m(\mu^+\mu^-) = 342\,\text{GeV}$, approximately $20\,\text{GeV}$ below the threshold required to detect both protons.

In the e^+e^- channel, a total of 23 events are observed with $\xi(e^+e^-)$ within the CT–PPS acceptance, and at least one track detected in the relevant RPs. Fifteen of those events have a mismatch of $\geq 2\sigma$ between $\xi(RP)$ and $\xi(e^+e^-)$ compared to the expectation of 10.5 ± 2.1 (stat+syst). Eight events have a scattered proton candidate in at least one of the two RPs matching $\xi(e^+e^-)$ within 2σ. The significance of observing 8 events with a background estimate of 2.36 ± 0.09 (stat) ± 0.47 (syst) is 2.6σ, including the systematic uncertainties profiled as log-normal nuisance parameters.

As for the dimuon case, no events in the e^+e^- channel are observed with matching protons in both arms, although the highest mass events are at $m(e^+e^-) = 650$ and $917\,\text{GeV}$, in the region where the double-arm acceptance is nonzero. Studies based on LPAIR indicate that less than one exclusive event is expected in this region for the integrated luminosity of the present data. The data show no activity compatible with a track in the RPs on the side where no proton is observed, thus ruling out track reconstruction problems. The expected ξ of the missing proton derived from the lepton kinematics corresponds to the detector region well outside the area suffering from inefficiencies induced by radiation damage. The two events observed are thus likely to be semiexclusive events, or background events with an uncorrelated proton.

Central semiexclusive dilepton events are expected to have very small values of $|t|$, the absolute value of the four-momentum squared exchanged at the proton vertices. As mentioned earlier, only the vertical component of the scattering angle, and hence of the proton transverse momentum, is currently measured. For 11 candidate dimuon events out of the 12, the vertical component of the scattering angle is compatible with zero within at most $2.5\,\sigma$, where σ is the uncertainty of the vertical component of the scattering angle. For one event, the discrepancy is $3.5\,\sigma$, in agreement with the background estimate. Also for the dielectron data the vertical component of the scattering angle, and hence of the proton transverse momentum, is measured; it is consistent with zero, as expected for the signal, for six of the eight events. Two events have values more than $3\,\sigma$ away from zero. This is again consistent with the background estimate. The vertical component of the scattering angle for the two highest-mass e^+e^- events is compatible with zero.

The correlation of $\xi(\ell^+\ell^-)$ versus $\xi(\text{RP})$ and the mass versus rapidity distributions, for the combined dimuon and dielectron results, are shown in Figs. 11 and 12. The combined signal significance is estimated by performing pseudo-experiments according to a joint distribution, including systematic uncertainties, and corresponds to an excess of $5.1\,\sigma$ over the background. In the calculation, the uncertainty on the integrated luminosity and that on the rapidity gap survival probability are assumed to be fully correlated between the two channels. All other sources are taken as independent. Of the 20 total events selected, 13 have a track in both the near and far RPs. In these events, the two independent ξ measurements agree within 4%.

The fractions of the exclusive and single proton dissociative contributions in the final sample of matching events are estimated by comparing their acoplanarity distribution to those expected for the two classes of events in LPAIR. This results in a contribution of approximately 70% from single proton dissociation, consistent within large uncertainties with the predictions of LPAIR weighted by the rapidity gap survival probabilities. The dominance of single dissociation is also consistent with the lack of a second observed proton in the two high-mass e^+e^- events.

The observed yields are consistent with those predicted by LPAIR modified by the rapidity gap survival probabilities, assuming the fraction of single proton dissociation events from the acoplanarity comparison just discussed. The full simulation of the CMS central apparatus (Section 5) is used. For the scattered protons, the prediction includes the effect of the CT–PPS acceptance, that of radiation damage in the silicon strip sensors, and the inefficiency due to multiple proton tracks. The comparison is performed in the region where radiation damage is less severe, corresponding to $\xi(\text{RP}) \geq 0.05$.

9   Summary

We have studied $\gamma\gamma \to \mu^+\mu^-$ and $\gamma\gamma \to e^+e^-$ production together with forward protons reconstructed in the CMS–TOTEM precision proton spectrometer (CT–PPS), using a sample
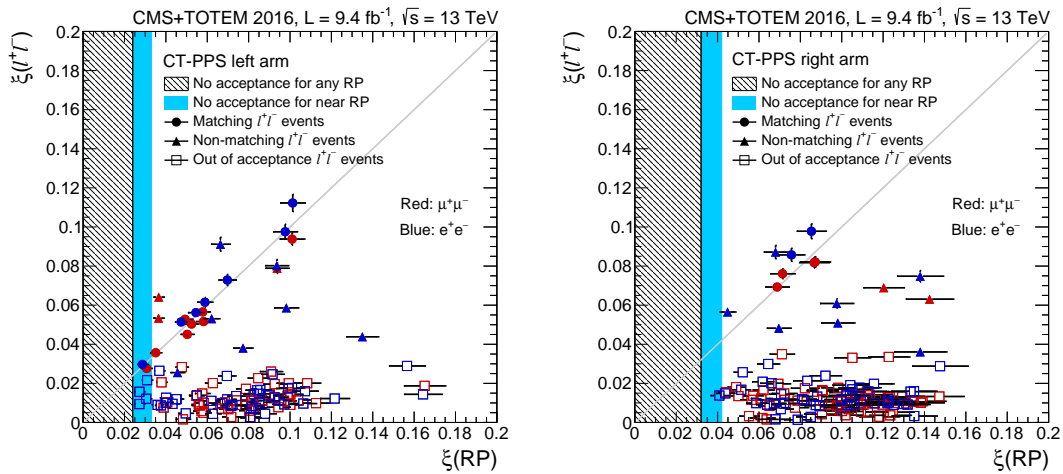
Figure 11: Correlation between the fractional values of the proton momentum loss measured in the central dilepton system, $\xi(\ell^+\ell^-)$, and in the RPs, $\xi(RP)$, for both RPs in each arm combined. The 45 (left) and 56 (right) arms are shown. The hatched region corresponds to the kinematical region outside the acceptance of both the near and far RPs, while the shaded (pale blue) region corresponds to the region outside the acceptance of the near RP. For the events in which a track is detected in both, the ξ value measured at the near RP is plotted. The horizontal error bars indicate the uncertainty of $\xi(RP)$, and the vertical bars the uncertainty of $\xi(\ell^+\ell^-)$. The events labeled "out of acceptance" are those in which $\xi(\ell^+\ell^-)$ corresponds to a signal proton outside the RP acceptance; in these events a background proton is detected with nonmatching kinematics.
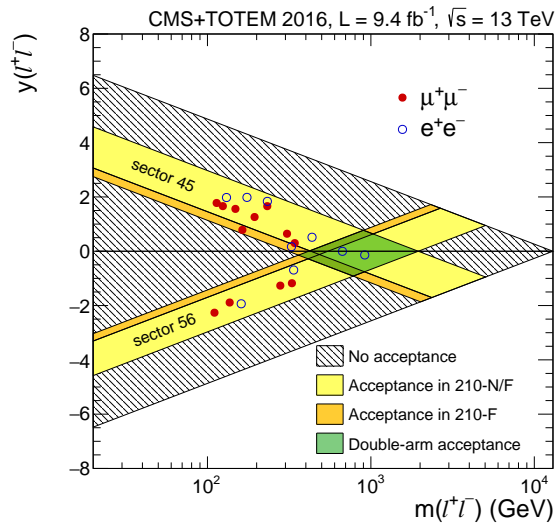
Figure 12: Expected acceptance regions in the rapidity vs. invariant mass plane overlaid with the observed dimuon (closed circles) and dielectron (open circles) signal candidate events. The "double-arm acceptance" refers to exclusive events, $pp \rightarrow p\ell^+\ell^-p$. Following the CMS convention, the positive (negative) rapidity region corresponds to the 45 (56) LHC sector.

of $9.4\,\mathrm{fb}^{-1}$ collected in proton–proton collisions at $\sqrt{s} = 13\,\mathrm{TeV}$. The Roman Pot alignment and LHC optics corrections have been determined using a high statistics sample of forward protons. A total of 12 $\gamma\gamma \rightarrow \mu^+\mu^-$ and 8 $\gamma\gamma \rightarrow e^+e^-$ events are observed with dilepton invariant mass larger than $110\,\mathrm{GeV}$, and a forward proton with consistent kinematics. This corresponds to an excess larger than five standard deviations over the expected background from

double-dissociative and Drell–Yan dilepton processes. The result represents the first observation of proton-tagged $\gamma\gamma$ collisions at the electroweak scale. The present data demonstrate the excellent performance of CT–PPS and its potential for high-mass exclusive (proton-tagged) measurements. With its 2016 operation, CT–PPS has proven for the first time the feasibility of continuously operating a near-beam proton spectrometer at a high-luminosity hadron collider.

Acknowledgments

References

[1] J. de Favereau de Jeneret et al., "High energy photon interactions at the LHC", (2009). `arXiv:0908.2020`.

[2] D. d'Enterria, M. Klasen, and K. Piotrzkowski, eds., "High-energy photon collisions at the LHC. Proceedings, International Workshop, Photon-LHC-2008, Geneva, Switzerland, 2008", volume 179-180. (2008).

[3] CMS Collaboration, "Study of exclusive two-photon production of W^+W^- in pp collisions at $\sqrt{s} = 7$ TeV and constraints on anomalous quartic gauge couplings", *JHEP* **07** (2013) 116, `doi:10.1007/JHEP07(2013)116`, `arXiv:1305.5596`.

[4] CMS Collaboration, "Evidence for exclusive $\gamma\gamma \to W^+W^-$ production and constraints on anomalous quartic gauge couplings in pp collisions at $\sqrt{s} = 7$ and 8 TeV", *JHEP* **08** (2016) 119, `doi:10.1007/JHEP08(2016)119`, `arXiv:1604.04464`.

[5] ATLAS Collaboration, "Measurement of exclusive $\gamma\gamma \to W^+W^-$ production and search for exclusive Higgs boson production in pp collisions at $\sqrt{s} = 8$ TeV using the ATLAS detector", *Phys. Rev. D* **94** (2016) 032011, `doi:10.1103/PhysRevD.94.032011`, `arXiv:1607.03745`.

[6] S. Atag, S. C. Inan, and I. Sahin, "Extra dimensions in photon-induced two lepton final states at the CERN-LHC", *Phys. Rev. D* **80** (2009) 075009, `doi:10.1103/PhysRevD.80.075009`, `arXiv:0904.2687`.

[7] I. Sahin and S. C. Inan, "Probe of unparticles at the LHC in exclusive two lepton and two photon production via photon-photon fusion", *JHEP* **09** (2009) 069, `doi:10.1088/1126-6708/2009/09/069`, `arXiv:0907.3290`.

[8] S. C. Inan, "Exclusive excited leptons search in two lepton final states at the CERN-LHC", *Phys. Rev. D* **81** (2010) 115002, `doi:10.1103/PhysRevD.81.115002`, `arXiv:1005.3432`.

[9] CDF Collaboration, "Observation of exclusive electron-positron production in hadron-hadron collisions", *Phys. Rev. Lett.* **98** (2007) 112001, `doi:10.1103/PhysRevLett.98.112001`, `arXiv:hep-ex/0611040`.

[10] CDF Collaboration, "Search for exclusive Z boson production and observation of high mass $p\bar{p} \to \gamma\gamma \to p + \ell\ell + \bar{p}$ events in $p\bar{p}$ collisions at $\sqrt{s}$ = 1.96 TeV", *Phys. Rev. Lett.* **102** (2009) 222002, `doi:10.1103/PhysRevLett.102.222002`, `arXiv:0902.2816`.

[11] CMS Collaboration, "Exclusive photon-photon production of muon pairs in proton-proton collisions at $\sqrt{s} = 7$ TeV", *JHEP* **01** (2012) 052, `doi:10.1007/JHEP01(2012)052`, `arXiv:1111.5536`.

[12] CMS Collaboration, "Search for exclusive or semi-exclusive photon pair production and observation of exclusive and semi-exclusive electron pair production in pp collisions at $\sqrt{s} = 7$ TeV", *JHEP* **11** (2012) 080, `doi:10.1007/JHEP11(2012)080`, `arXiv:1209.1666`.

[13] ATLAS Collaboration, "Measurement of exclusive $\gamma\gamma \to \ell^+\ell^-$ production in proton-proton collisions at $\sqrt{s} = 7$ TeV with the ATLAS detector", *Phys. Lett. B* **749** (2015) 242, `doi:10.1016/j.physletb.2015.07.069`, `arXiv:1506.07098`.

[14] ATLAS Collaboration, "Measurement of the exclusive $\gamma\gamma \to \mu^+\mu^-$ process in proton-proton collisions at $\sqrt{s} = 13$ TeV with the ATLAS detector", *Phys. Lett. B* **777** (2018) 303, `doi:10.1016/j.physletb.2017.12.043`, `arXiv:1708.04053`.

[15] CMS and TOTEM Collaborations, "CMS-TOTEM Precision Proton Spectrometer", Technical Report CERN-LHCC-2014-021. TOTEM-TDR-003. CMS-TDR-13, 2014.

[16] G. Ruggiero et al., "Characteristics of edgeless silicon detectors for the Roman pots of the TOTEM experiment at the LHC", *Nucl. Instrum. Meth. A* **604** (2009) 242, `doi:10.1016/j.nima.2009.01.056`.

[17] CMS Collaboration, "The CMS experiment at the CERN LHC", *JINST* **3** (2008) S08004, `doi:10.1088/1748-0221/3/08/S08004`.

[18] J. Kaplon and W. Dabrowski, "Fast CMOS binary front end for silicon strip detectors at LHC experiments", *IEEE Trans. Nucl. Sci.* **52** (2005) 2713, `doi:10.1109/TNS.2005.862826`.

[19] TOTEM Collaboration, "Performance of the TOTEM detectors at the LHC", *Int. J. Mod. Phys. A* **28** (2013) 1330046, `doi:10.1142/S0217751X13300469`, `arXiv:1310.2908`.

[20] J. Kaspar, "Alignment of CT-PPS detectors in 2016, before TS2", CERN-TOTEM-NOTE 2017-001, 2017.

[21] F. Nemes, "LHC optics determination with proton tracks measured in the CT-PPS detectors in 2016, before TS2", CERN-TOTEM-NOTE CERN-TOTEM-NOTE-2017-002, 2017.

[22] H. Grote and F. Schmidt, "MAD-X: An upgrade from MAD8", in *2003 Particle Accelerator Conference*. Portland, Oregon, May, 2003. econf C03-05-12.

[23] TOTEM Collaboration, "LHC optics measurement with proton tracks detected by the Roman pots of the TOTEM experiment", *New J. Phys.* **16** (2014) 103041, `doi:10.1088/1367-2630/16/10/103041`, `arXiv:1406.0546`.

[24] J. Kaspar, "Elastic scattering at the LHC". PhD thesis, Prague, Inst. Phys., 2011. CERN-THESIS-2011-214.

[25] J. A. M. Vermaseren, "Two photon processes at very high energies", *Nucl. Phys. B* **229** (1983) 347, `doi:10.1016/0550-3213(83)90336-X`.

[26] S. P. Baranov, O. Dünger, H. Shooshtari, and J. A. M. Vermaseren, "LPAIR: A generator for lepton pair production", in *Workshop on Physics at HERA Hamburg, Germany, October 29-30, 1991*, p. 1478. 1991.

[27] GEANT4 Collaboration, "GEANT4—a simulation toolkit", *Nucl. Instrum. Meth. A* **506** (2003) 250, `doi:10.1016/S0168-9002(03)01368-8`.

[28] J. Alwall et al., "The automated computation of tree-level and next-to-leading order differential cross sections, and their matching to parton shower simulations", *JHEP* **07** (2014) 079, `doi:10.1007/JHEP07(2014)079`, `arXiv:1405.0301`.

[29] R. Frederix and S. Frixione, "Merging meets matching in MC@NLO", *JHEP* **12** (2012) 061, `doi:10.1007/JHEP12(2012)061`, `arXiv:1209.6215`.

[30] T. Sjöstrand, S. Mrenna, and P. Z. Skands, "A brief introduction to PYTHIA 8.1", *Comput. Phys. Commun.* **178** (2008) 852, `doi:10.1016/j.cpc.2008.01.036`, `arXiv:0710.3820`.

[31] CMS Collaboration, "Event generator tunes obtained from underlying event and multiparton scattering measurements", *Eur. Phys. J. C* **76** (2016) 155, `doi:10.1140/epjc/s10052-016-3988-x`, `arXiv:1512.00815`.

[32] Y. Li and F. Petriello, "Combining QCD and electroweak corrections to dilepton production in FEWZ", *Phys. Rev. D* **86** (2012) 094034, `doi:10.1103/PhysRevD.86.094034`, `arXiv:1208.5967`.

[33] CMS Collaboration, "The CMS trigger system", *JINST* **12** (2017) P01020, `doi:10.1088/1748-0221/12/01/P01020`, `arXiv:1609.02366`.

[34] CMS Collaboration, "Performance of CMS muon reconstruction in pp collision events at $\sqrt{s} = 7$ TeV", *JINST* **7** (2012) P10002, `doi:10.1088/1748-0221/7/10/P10002`, `arXiv:1206.4071`.

[35] CMS Collaboration, "Performance of electron reconstruction and selection with the CMS detector in proton-proton collisions at $\sqrt{s} = 8$ TeV", *JINST* **10** (2015) P06005, `doi:10.1088/1748-0221/10/06/P06005`, `arXiv:1502.02701`.

[36] CDF Collaboration, "Observation of exclusive charmonium production and $\gamma + \gamma$ to $\mu^+\mu^-$ in $p\bar{p}$ collisions at $\sqrt{s} = 1.96$ TeV", *Phys. Rev. Lett.* **102** (2009) 242001, `doi:10.1103/PhysRevLett.102.242001`, `arXiv:0902.1271`.

[37] L. A. Harland-Lang, V. A. Khoze, and M. G. Ryskin, "The photon PDF in events with rapidity gaps", *Eur. Phys. J. C* **76** (2016) 255, `doi:10.1140/epjc/s10052-016-4100-2`, `arXiv:1601.03772`.

[38] M. Dyndal and L. Schoeffel, "The role of finite-size effects on the spectrum of equivalent photons in proton-proton collisions at the LHC", *Phys. Lett. B* **741** (2015) 66, `doi:10.1016/j.physletb.2014.12.019`, `arXiv:1410.2983`.

[39] L. A. Harland-Lang, V. A. Khoze, and M. G. Ryskin, "Exclusive physics at the LHC with SuperChic 2", *Eur. Phys. J. C* **76** (2016) 9, `doi:10.1140/epjc/s10052-015-3832-8`, `arXiv:1508.02718`.

[40] CMS Collaboration, "CMS luminosity measurements for the 2016 data-taking period", CMS Physics Analysis Summary CMS-PAS-LUM-17-001, 2017.

A The CMS Collaboration

Yerevan Physics Institute, Yerevan, Armenia
A.M. Sirunyan, A. Tumasyan

Institut für Hochenergiephysik, Wien, Austria
W. Adam, F. Ambrogi, E. Asilar, T. Bergauer, J. Brandstetter, E. Brondolin, M. Dragicevic, J. Erö, A. Escalante Del Valle, M. Flechl, M. Friedl, R. Frühwirth[1], V.M. Ghete, J. Grossmann, J. Hrubec, M. Jeitler[1], A. König, N. Krammer, I. Krätschmer, D. Liko, T. Madlener, I. Mikulec, E. Pree, N. Rad, H. Rohringer, J. Schieck[1], R. Schöfbeck, M. Spanring, D. Spitzbart, A. Taurok, W. Waltenberger, J. Wittmann, C.-E. Wulz[1], M. Zarucki

Institute for Nuclear Problems, Minsk, Belarus
V. Chekhovsky, V. Mossolov, J. Suarez Gonzalez

Universiteit Antwerpen, Antwerpen, Belgium
E.A. De Wolf, D. Di Croce, X. Janssen, J. Lauwers, M. Pieters, M. Van De Klundert, H. Van Haevermaet, P. Van Mechelen, N. Van Remortel

Vrije Universiteit Brussel, Brussel, Belgium
S. Abu Zeid, F. Blekman, J. D'Hondt, I. De Bruyn, J. De Clercq, K. Deroover, G. Flouris, D. Lontkovskyi, S. Lowette, I. Marchesini, S. Moortgat, L. Moreels, Q. Python, K. Skovpen, S. Tavernier, W. Van Doninck, P. Van Mulders, I. Van Parijs

Université Libre de Bruxelles, Bruxelles, Belgium
D. Beghin, B. Bilin, H. Brun, B. Clerbaux, G. De Lentdecker, H. Delannoy, B. Dorney, G. Fasanella, L. Favart, R. Goldouzian, A. Grebenyuk, A.K. Kalsi, T. Lenzi, J. Luetic, T. Seva, E. Starling, C. Vander Velde, P. Vanlaer, D. Vannerom, R. Yonamine

Ghent University, Ghent, Belgium
T. Cornelis, D. Dobur, A. Fagot, M. Gul, I. Khvastunov[2], D. Poyraz, C. Roskas, D. Trocino, M. Tytgat, W. Verbeke, B. Vermassen, M. Vit, N. Zaganidis

Université Catholique de Louvain, Louvain-la-Neuve, Belgium
H. Bakhshiansohi, O. Bondu, S. Brochet, G. Bruno, C. Caputo, A. Caudron, P. David, S. De Visscher, C. Delaere, M. Delcourt, B. Francois, A. Giammanco, G. Krintiras, V. Lemaitre, A. Magitteri, A. Mertens, M. Musich, K. Piotrzkowski, L. Quertenmont, A. Saggio, M. Vidal Marono, S. Wertz, J. Zobec

Centro Brasileiro de Pesquisas Fisicas, Rio de Janeiro, Brazil
W.L. Aldá Júnior, F.L. Alves, G.A. Alves, L. Brito, G. Correia Silva, C. Hensel, A. Moraes, M.E. Pol, P. Rebello Teles

Universidade do Estado do Rio de Janeiro, Rio de Janeiro, Brazil
E. Belchior Batista Das Chagas, W. Carvalho, J. Chinellato[3], E. Coelho, E.M. Da Costa, G.G. Da Silveira[4], D. De Jesus Damiao, S. Fonseca De Souza, H. Malbouisson, M. Medina Jaime[5], M. Melo De Almeida, C. Mora Herrera, L. Mundim, H. Nogima, L.J. Sanchez Rosas, A. Santoro, A. Sznajder, M. Thiel, E.J. Tonelli Manganote[3], F. Torres Da Silva De Araujo, A. Vilela Pereira

Universidade Estadual Paulista [a], Universidade Federal do ABC [b], São Paulo, Brazil
S. Ahuja[a], C.A. Bernardes[a], L. Calligaris[a], T.R. Fernandez Perez Tomei[a], E.M. Gregores[b], P.G. Mercadante[b], S.F. Novaes[a], Sandra S. Padula[a], D. Romero Abad[b], J.C. Ruiz Vargas[a]

Institute for Nuclear Research and Nuclear Energy, Bulgarian Academy of Sciences, Sofia, Bulgaria
A. Aleksandrov, R. Hadjiiska, P. Iaydjiev, A. Marinov, M. Misheva, M. Rodozov, M. Shopova, G. Sultanov

University of Sofia, Sofia, Bulgaria
A. Dimitrov, L. Litov, B. Pavlov, P. Petkov

Beihang University, Beijing, China
W. Fang[6], X. Gao[6], L. Yuan

Institute of High Energy Physics, Beijing, China
M. Ahmad, J.G. Bian, G.M. Chen, H.S. Chen, M. Chen, Y. Chen, C.H. Jiang, D. Leggat, H. Liao, Z. Liu, F. Romeo, S.M. Shaheen, A. Spiezia, J. Tao, C. Wang, Z. Wang, E. Yazgan, H. Zhang, J. Zhao

State Key Laboratory of Nuclear Physics and Technology, Peking University, Beijing, China
Y. Ban, G. Chen, J. Li, Q. Li, S. Liu, Y. Mao, S.J. Qian, D. Wang, Z. Xu

Tsinghua University, Beijing, China
Y. Wang

Universidad de Los Andes, Bogota, Colombia
C. Avila, A. Cabrera, C.A. Carrillo Montoya, L.F. Chaparro Sierra, C. Florez, C.F. González Hernández, M.A. Segura Delgado

University of Split, Faculty of Electrical Engineering, Mechanical Engineering and Naval Architecture, Split, Croatia
B. Courbon, N. Godinovic, D. Lelas, I. Puljak, P.M. Ribeiro Cipriano, T. Sculac

University of Split, Faculty of Science, Split, Croatia
Z. Antunovic, M. Kovac

Institute Rudjer Boskovic, Zagreb, Croatia
V. Brigljevic, D. Ferencek, K. Kadija, B. Mesic, A. Starodumov[7], T. Susa

University of Cyprus, Nicosia, Cyprus
M.W. Ather, A. Attikis, G. Mavromanolakis, J. Mousa, C. Nicolaou, F. Ptochos, P.A. Razis, H. Rykaczewski

Charles University, Prague, Czech Republic
M. Finger[8], M. Finger Jr.[8]

Universidad San Francisco de Quito, Quito, Ecuador
E. Carrera Jarrin

Academy of Scientific Research and Technology of the Arab Republic of Egypt, Egyptian Network of High Energy Physics, Cairo, Egypt
A. Ellithi Kamel[9], A. Mohamed[10], E. Salama[11,12]

National Institute of Chemical Physics and Biophysics, Tallinn, Estonia
S. Bhowmik, R.K. Dewanjee, M. Kadastik, L. Perrini, M. Raidal, C. Veelken

Department of Physics, University of Helsinki, Helsinki, Finland
P. Eerola, H. Kirschenmann, J. Pekkanen, M. Voutilainen

Helsinki Institute of Physics, Helsinki, Finland
J. Havukainen, J.K. Heikkilä, T. Järvinen, V. Karimäki, R. Kinnunen, T. Lampén, K. Lassila-Perini, S. Laurila, S. Lehti, T. Lindén, P. Luukka, T. Mäenpää, H. Siikonen, E. Tuominen, J. Tuominiemi

Lappeenranta University of Technology, Lappeenranta, Finland
T. Tuuva

IRFU, CEA, Université Paris-Saclay, Gif-sur-Yvette, France
M. Besancon, F. Couderc, M. Dejardin, D. Denegri, J.L. Faure, F. Ferri, S. Ganjour, S. Ghosh, A. Givernaud, P. Gras, G. Hamel de Monchenault, P. Jarry, C. Leloup, E. Locci, M. Machet, J. Malcles, G. Negro, J. Rander, A. Rosowsky, M.Ö. Sahin, M. Titov

Laboratoire Leprince-Ringuet, Ecole polytechnique, CNRS/IN2P3, Université Paris-Saclay, Palaiseau, France
A. Abdulsalam[13], C. Amendola, I. Antropov, S. Baffioni, F. Beaudette, P. Busson, L. Cadamuro, C. Charlot, R. Granier de Cassagnac, M. Jo, I. Kucher, S. Lisniak, A. Lobanov, J. Martin Blanco, M. Nguyen, C. Ochando, G. Ortona, P. Paganini, P. Pigard, R. Salerno, J.B. Sauvan, Y. Sirois, A.G. Stahl Leiton, Y. Yilmaz, A. Zabi, A. Zghiche

Université de Strasbourg, CNRS, IPHC UMR 7178, F-67000 Strasbourg, France
J.-L. Agram[14], J. Andrea, D. Bloch, J.-M. Brom, E.C. Chabert, C. Collard, E. Conte[14], X. Coubez, F. Drouhin[14], J.-C. Fontaine[14], D. Gelé, U. Goerlach, M. Jansová, P. Juillot, A.-C. Le Bihan, N. Tonon, P. Van Hove

Centre de Calcul de l'Institut National de Physique Nucleaire et de Physique des Particules, CNRS/IN2P3, Villeurbanne, France
S. Gadrat

Université de Lyon, Université Claude Bernard Lyon 1, CNRS-IN2P3, Institut de Physique Nucléaire de Lyon, Villeurbanne, France
S. Beauceron, C. Bernet, G. Boudoul, N. Chanon, R. Chierici, D. Contardo, P. Depasse, H. El Mamouni, J. Fay, L. Finco, S. Gascon, M. Gouzevitch, G. Grenier, B. Ille, F. Lagarde, I.B. Laktineh, H. Lattaud, M. Lethuillier, L. Mirabito, A.L. Pequegnot, S. Perries, A. Popov[15], V. Sordini, M. Vander Donckt, S. Viret, S. Zhang

Georgian Technical University, Tbilisi, Georgia
T. Toriashvili[16]

Tbilisi State University, Tbilisi, Georgia
Z. Tsamalaidze[8]

RWTH Aachen University, I. Physikalisches Institut, Aachen, Germany
C. Autermann, L. Feld, M.K. Kiesel, K. Klein, M. Lipinski, M. Preuten, M.P. Rauch, C. Schomakers, J. Schulz, M. Teroerde, B. Wittmer, V. Zhukov[15]

RWTH Aachen University, III. Physikalisches Institut A, Aachen, Germany
A. Albert, D. Duchardt, M. Endres, M. Erdmann, S. Erdweg, T. Esch, R. Fischer, A. Güth, T. Hebbeker, C. Heidemann, K. Hoepfner, S. Knutzen, M. Merschmeyer, A. Meyer, P. Millet, S. Mukherjee, T. Pook, M. Radziej, H. Reithler, M. Rieger, F. Scheuch, D. Teyssier, S. Thüer

RWTH Aachen University, III. Physikalisches Institut B, Aachen, Germany
G. Flügge, B. Kargoll, T. Kress, A. Künsken, T. Müller, A. Nehrkorn, A. Nowack, C. Pistone, O. Pooth, A. Stahl[17]

Deutsches Elektronen-Synchrotron, Hamburg, Germany
M. Aldaya Martin, T. Arndt, C. Asawatangtrakuldee, K. Beernaert, O. Behnke, U. Behrens, A. Bermúdez Martínez, A.A. Bin Anuar, K. Borras[18], V. Botta, A. Campbell, P. Connor, C. Contreras-Campana, F. Costanza, V. Danilov, A. De Wit, C. Diez Pardos, D. Domínguez Damiani, G. Eckerlin, D. Eckstein, T. Eichhorn, E. Eren, E. Gallo[19], J. Garay Garcia, A. Geiser, J.M. Grados Luyando, A. Grohsjean, P. Gunnellini, M. Guthoff, A. Harb, J. Hauk, M. Hempel[20], H. Jung, M. Kasemann, J. Keaveney, C. Kleinwort, J. Knolle, I. Korol, D. Krücker, W. Lange, A. Lelek, T. Lenz, K. Lipka, W. Lohmann[20], R. Mankel, I.-A. Melzer-Pellmann, A.B. Meyer, M. Meyer, M. Missiroli, G. Mittag, J. Mnich, A. Mussgiller, D. Pitzl, A. Raspereza, M. Savitskyi, P. Saxena, R. Shevchenko, N. Stefaniuk, H. Tholen, G.P. Van Onsem, R. Walsh, Y. Wen, K. Wichmann, C. Wissing, O. Zenaiev

University of Hamburg, Hamburg, Germany
R. Aggleton, S. Bein, V. Blobel, M. Centis Vignali, T. Dreyer, E. Garutti, D. Gonzalez, J. Haller, A. Hinzmann, M. Hoffmann, A. Karavdina, G. Kasieczka, R. Klanner, R. Kogler, N. Kovalchuk, S. Kurz, D. Marconi, J. Multhaup, M. Niedziela, D. Nowatschin, T. Peiffer, A. Perieanu, A. Reimers, C. Scharf, P. Schleper, A. Schmidt, S. Schumann, J. Schwandt, J. Sonneveld, H. Stadie, G. Steinbrück, F.M. Stober, M. Stöver, D. Troendle, E. Usai, A. Vanhoefer, B. Vormwald

Institut für Experimentelle Teilchenphysik, Karlsruhe, Germany
M. Akbiyik, C. Barth, M. Baselga, S. Baur, E. Butz, R. Caspart, T. Chwalek, F. Colombo, W. De Boer, A. Dierlamm, N. Faltermann, B. Freund, R. Friese, M. Giffels, M.A. Harrendorf, F. Hartmann[17], S.M. Heindl, U. Husemann, F. Kassel[17], S. Kudella, H. Mildner, M.U. Mozer, Th. Müller, M. Plagge, G. Quast, K. Rabbertz, M. Schröder, I. Shvetsov, G. Sieber, H.J. Simonis, R. Ulrich, S. Wayand, M. Weber, T. Weiler, S. Williamson, C. Wöhrmann, R. Wolf

Institute of Nuclear and Particle Physics (INPP), NCSR Demokritos, Aghia Paraskevi, Greece
G. Anagnostou, G. Daskalakis, T. Geralis, A. Kyriakis, D. Loukas, I. Topsis-Giotis

National and Kapodistrian University of Athens, Athens, Greece
G. Karathanasis, S. Kesisoglou, A. Panagiotou, N. Saoulidou, E. Tziaferi

National Technical University of Athens, Athens, Greece
K. Kousouris, I. Papakrivopoulos

University of Ioánnina, Ioánnina, Greece
I. Evangelou, C. Foudas, P. Gianneios, P. Katsoulis, P. Kokkas, S. Mallios, N. Manthos, I. Papadopoulos, E. Paradas, J. Strologas, F.A. Triantis, D. Tsitsonis

MTA-ELTE Lendület CMS Particle and Nuclear Physics Group, Eötvös Loránd University, Budapest, Hungary
M. Csanad, N. Filipovic, G. Pasztor, O. Surányi, G.I. Veres[21]

Wigner Research Centre for Physics, Budapest, Hungary
G. Bencze, C. Hajdu, D. Horvath[22], Á. Hunyadi, F. Sikler, T.Á. Vámi, V. Veszpremi, G. Vesztergombi[21]

Institute of Nuclear Research ATOMKI, Debrecen, Hungary
N. Beni, S. Czellar, J. Karancsi[23], A. Makovec, J. Molnar, Z. Szillasi

Institute of Physics, University of Debrecen, Debrecen, Hungary
M. Bartók[21], P. Raics, Z.L. Trocsanyi, B. Ujvari

Indian Institute of Science (IISc), Bangalore, India
S. Choudhury, J.R. Komaragiri

National Institute of Science Education and Research, Bhubaneswar, India
S. Bahinipati[24], P. Mal, K. Mandal, A. Nayak[25], D.K. Sahoo[24], S.K. Swain

Panjab University, Chandigarh, India
S. Bansal, S.B. Beri, V. Bhatnagar, S. Chauhan, R. Chawla, N. Dhingra, R. Gupta, A. Kaur, M. Kaur, S. Kaur, R. Kumar, P. Kumari, M. Lohan, A. Mehta, S. Sharma, J.B. Singh, G. Walia

University of Delhi, Delhi, India
A. Bhardwaj, B.C. Choudhary, R.B. Garg, S. Keshri, A. Kumar, Ashok Kumar, S. Malhotra, M. Naimuddin, K. Ranjan, Aashaq Shah, R. Sharma

Saha Institute of Nuclear Physics, HBNI, Kolkata, India
R. Bhardwaj[26], R. Bhattacharya, S. Bhattacharya, U. Bhawandeep[26], D. Bhowmik, S. Dey, S. Dutt[26], S. Dutta, S. Ghosh, N. Majumdar, K. Mondal, S. Mukhopadhyay, S. Nandan, A. Purohit, P.K. Rout, A. Roy, S. Roy Chowdhury, S. Sarkar, M. Sharan, B. Singh, S. Thakur[26]

Indian Institute of Technology Madras, Madras, India
P.K. Behera

Bhabha Atomic Research Centre, Mumbai, India
R. Chudasama, D. Dutta, V. Jha, V. Kumar, A.K. Mohanty[17], P.K. Netrakanti, L.M. Pant, P. Shukla, A. Topkar

Tata Institute of Fundamental Research-A, Mumbai, India
T. Aziz, S. Dugad, B. Mahakud, S. Mitra, G.B. Mohanty, N. Sur, B. Sutar

Tata Institute of Fundamental Research-B, Mumbai, India
S. Banerjee, S. Bhattacharya, S. Chatterjee, P. Das, M. Guchait, Sa. Jain, S. Kumar, M. Maity[27], G. Majumder, K. Mazumdar, N. Sahoo, T. Sarkar[27], N. Wickramage[28]

Indian Institute of Science Education and Research (IISER), Pune, India
S. Chauhan, S. Dube, V. Hegde, A. Kapoor, K. Kothekar, S. Pandey, A. Rane, S. Sharma

Institute for Research in Fundamental Sciences (IPM), Tehran, Iran
S. Chenarani[29], E. Eskandari Tadavani, S.M. Etesami[29], M. Khakzad, M. Mohammadi Najafabadi, M. Naseri, S. Paktinat Mehdiabadi[30], F. Rezaei Hosseinabadi, B. Safarzadeh[31], M. Zeinali

University College Dublin, Dublin, Ireland
M. Felcini, M. Grunewald

INFN Sezione di Bari [a], Università di Bari [b], Politecnico di Bari [c], Bari, Italy
M. Abbrescia[a,b], C. Calabria[a,b], A. Colaleo[a], D. Creanza[a,c], L. Cristella[a,b], N. De Filippis[a,c], M. De Palma[a,b], A. Di Florio[a,b], F. Errico[a,b], L. Fiore[a], A. Gelmi[a,b], G. Iaselli[a,c], S. Lezki[a,b], G. Maggi[a,c], M. Maggi[a], B. Marangelli[a,b], G. Miniello[a,b], S. My[a,b], S. Nuzzo[a,b], A. Pompili[a,b], G. Pugliese[a,c], R. Radogna[a], A. Ranieri[a], G. Selvaggi[a,b], A. Sharma[a], L. Silvestris[a,17], R. Venditti[a], P. Verwilligen[a], G. Zito[a]

INFN Sezione di Bologna [a], Università di Bologna [b], Bologna, Italy
G. Abbiendi[a], C. Battilana[a,b], D. Bonacorsi[a,b], L. Borgonovi[a,b], S. Braibant-Giacomelli[a,b], R. Campanini[a,b], P. Capiluppi[a,b], A. Castro[a,b], F.R. Cavallo[a], S.S. Chhibra[a,b], G. Codispoti[a,b], M. Cuffiani[a,b], G.M. Dallavalle[a], F. Fabbri[a], A. Fanfani[a,b], D. Fasanella[a,b], P. Giacomelli[a],

C. Grandi[a], L. Guiducci[a,b], F. Iemmi, S. Marcellini[a], G. Masetti[a], A. Montanari[a], F.L. Navarria[a,b], A. Perrotta[a], A.M. Rossi[a,b], T. Rovelli[a,b], G.P. Siroli[a,b], N. Tosi[a]

INFN Sezione di Catania [a], **Università di Catania** [b], **Catania, Italy**
S. Albergo[a,b], S. Costa[a,b], A. Di Mattia[a], F. Giordano[a,b], R. Potenza[a,b], A. Tricomi[a,b], C. Tuve[a,b]

INFN Sezione di Firenze [a], **Università di Firenze** [b], **Firenze, Italy**
G. Barbagli[a], K. Chatterjee[a,b], V. Ciulli[a,b], C. Civinini[a], R. D'Alessandro[a,b], E. Focardi[a,b], G. Latino, P. Lenzi[a,b], M. Meschini[a], S. Paoletti[a], L. Russo[a,32], G. Sguazzoni[a], D. Strom[a], L. Viliani[a]

INFN Laboratori Nazionali di Frascati, Frascati, Italy
L. Benussi, S. Bianco, F. Fabbri, D. Piccolo, F. Primavera[17]

INFN Sezione di Genova [a], **Università di Genova** [b], **Genova, Italy**
V. Calvelli[a,b], F. Ferro[a], F. Ravera[a,b], E. Robutti[a], S. Tosi[a,b]

INFN Sezione di Milano-Bicocca [a], **Università di Milano-Bicocca** [b], **Milano, Italy**
A. Benaglia[a], A. Beschi[b], L. Brianza[a,b], F. Brivio[a,b], V. Ciriolo[a,b,17], M.E. Dinardo[a,b], S. Fiorendi[a,b], S. Gennai[a], A. Ghezzi[a,b], P. Govoni[a,b], M. Malberti[a,b], S. Malvezzi[a], R.A. Manzoni[a,b], D. Menasce[a], L. Moroni[a], M. Paganoni[a,b], K. Pauwels[a,b], D. Pedrini[a], S. Pigazzini[a,b,33], S. Ragazzi[a,b], T. Tabarelli de Fatis[a,b]

INFN Sezione di Napoli [a], **Università di Napoli 'Federico II'** [b], **Napoli, Italy, Università della Basilicata** [c], **Potenza, Italy, Università G. Marconi** [d], **Roma, Italy**
S. Buontempo[a], N. Cavallo[a,c], S. Di Guida[a,d,17], F. Fabozzi[a,c], F. Fienga[a,b], G. Galati[a,b], A.O.M. Iorio[a,b], W.A. Khan[a], L. Lista[a], S. Meola[a,d,17], P. Paolucci[a,17], C. Sciacca[a,b], F. Thyssen[a], E. Voevodina[a,b]

INFN Sezione di Padova [a], **Università di Padova** [b], **Padova, Italy, Università di Trento** [c], **Trento, Italy**
P. Azzi[a], N. Bacchetta[a], L. Benato[a,b], D. Bisello[a,b], A. Boletti[a,b], R. Carlin[a,b], A. Carvalho Antunes De Oliveira[a,b], P. Checchia[a], P. De Castro Manzano[a], T. Dorigo[a], U. Dosselli[a], F. Gasparini[a,b], U. Gasparini[a,b], A. Gozzelino[a], S. Lacaprara[a], M. Margoni[a,b], A.T. Meneguzzo[a,b], N. Pozzobon[a,b], P. Ronchese[a,b], R. Rossin[a,b], F. Simonetto[a,b], A. Tiko, E. Torassa[a], M. Zanetti[a,b], P. Zotto[a,b], G. Zumerle[a,b]

INFN Sezione di Pavia [a], **Università di Pavia** [b], **Pavia, Italy**
A. Braghieri[a], A. Magnani[a], P. Montagna[a,b], S.P. Ratti[a,b], V. Re[a], M. Ressegotti[a,b], C. Riccardi[a,b], P. Salvini[a], I. Vai[a,b], P. Vitulo[a,b]

INFN Sezione di Perugia [a], **Università di Perugia** [b], **Perugia, Italy**
L. Alunni Solestizi[a,b], M. Biasini[a,b], G.M. Bilei[a], C. Cecchi[a,b], D. Ciangottini[a,b], L. Fanò[a,b], P. Lariccia[a,b], R. Leonardi[a,b], E. Manoni[a], G. Mantovani[a,b], V. Mariani[a,b], M. Menichelli[a], A. Rossi[a,b], A. Santocchia[a,b], D. Spiga[a]

INFN Sezione di Pisa [a], **Università di Pisa** [b], **Scuola Normale Superiore di Pisa** [c], **Pisa, Italy**
K. Androsov[a], P. Azzurri[a,17], G. Bagliesi[a], L. Bianchini[a], T. Boccali[a], L. Borrello, R. Castaldi[a], M.A. Ciocci[a,b], R. Dell'Orso[a], G. Fedi[a], L. Giannini[a,c], A. Giassi[a], M.T. Grippo[a,32], F. Ligabue[a,c], T. Lomtadze[a], E. Manca[a,c], G. Mandorli[a,c], A. Messineo[a,b], F. Palla[a], A. Rizzi[a,b], P. Spagnolo[a], R. Tenchini[a], G. Tonelli[a,b], A. Venturi[a], P.G. Verdini[a]

INFN Sezione di Roma [a], **Sapienza Università di Roma** [b], **Rome, Italy**
L. Barone[a,b], F. Cavallari[a], M. Cipriani[a,b], N. Daci[a], D. Del Re[a,b], E. Di Marco[a,b], M. Diemoz[a],

S. Gelli[a,b], E. Longo[a,b], B. Marzocchi[a,b], P. Meridiani[a], G. Organtini[a,b], F. Pandolfi[a], R. Paramatti[a,b], F. Preiato[a,b], S. Rahatlou[a,b], C. Rovelli[a], F. Santanastasio[a,b]

INFN Sezione di Torino [a], Università di Torino [b], Torino, Italy, Università del Piemonte Orientale [c], Novara, Italy
N. Amapane[a,b], R. Arcidiacono[a,c], S. Argiro[a,b], M. Arneodo[a,c], N. Bartosik[a], R. Bellan[a,b], C. Biino[a], N. Cartiglia[a], R. Castello[a,b], F. Cenna[a,b], M. Costa[a,b], R. Covarelli[a,b], A. Degano[a,b], N. Demaria[a], B. Kiani[a,b], C. Mariotti[a], S. Maselli[a], E. Migliore[a,b], V. Monaco[a,b], E. Monteil[a,b], M. Monteno[a], M.M. Obertino[a,b], L. Pacher[a,b], N. Pastrone[a], M. Pelliccioni[a], G.L. Pinna Angioni[a,b], A. Romero[a,b], M. Ruspa[a,c], R. Sacchi[a,b], K. Shchelina[a,b], V. Sola[a], A. Solano[a,b], A. Staiano[a]

INFN Sezione di Trieste [a], Università di Trieste [b], Trieste, Italy
S. Belforte[a], M. Casarsa[a], F. Cossutti[a], G. Della Ricca[a,b], A. Zanetti[a]

Kyungpook National University
D.H. Kim, G.N. Kim, M.S. Kim, J. Lee, S. Lee, S.W. Lee, C.S. Moon, Y.D. Oh, S. Sekmen, D.C. Son, Y.C. Yang

Chonnam National University, Institute for Universe and Elementary Particles, Kwangju, Korea
H. Kim, D.H. Moon, G. Oh

Hanyang University, Seoul, Korea
J.A. Brochero Cifuentes, J. Goh, T.J. Kim

Korea University, Seoul, Korea
S. Cho, S. Choi, Y. Go, D. Gyun, S. Ha, B. Hong, Y. Jo, Y. Kim, K. Lee, K.S. Lee, S. Lee, J. Lim, S.K. Park, Y. Roh

Seoul National University, Seoul, Korea
J. Almond, J. Kim, J.S. Kim, H. Lee, K. Lee, K. Nam, S.B. Oh, B.C. Radburn-Smith, S.h. Seo, U.K. Yang, H.D. Yoo, G.B. Yu

University of Seoul, Seoul, Korea
H. Kim, J.H. Kim, J.S.H. Lee, I.C. Park

Sungkyunkwan University, Suwon, Korea
Y. Choi, C. Hwang, J. Lee, I. Yu

Vilnius University, Vilnius, Lithuania
V. Dudenas, A. Juodagalvis, J. Vaitkus

National Centre for Particle Physics, Universiti Malaya, Kuala Lumpur, Malaysia
I. Ahmed, Z.A. Ibrahim, M.A.B. Md Ali[34], F. Mohamad Idris[35], W.A.T. Wan Abdullah, M.N. Yusli, Z. Zolkapli

Centro de Investigacion y de Estudios Avanzados del IPN, Mexico City, Mexico
Duran-Osuna, M. C., H. Castilla-Valdez, E. De La Cruz-Burelo, Ramirez-Sanchez, G., I. Heredia-De La Cruz[36], Rabadan-Trejo, R. I., R. Lopez-Fernandez, J. Mejia Guisao, Reyes-Almanza, R, A. Sanchez-Hernandez

Universidad Iberoamericana, Mexico City, Mexico
S. Carrillo Moreno, C. Oropeza Barrera, F. Vazquez Valencia

Benemerita Universidad Autonoma de Puebla, Puebla, Mexico
J. Eysermans, I. Pedraza, H.A. Salazar Ibarguen, C. Uribe Estrada

Universidad Autónoma de San Luis Potosí, San Luis Potosí, Mexico
A. Morelos Pineda

University of Auckland, Auckland, New Zealand
D. Krofcheck

University of Canterbury, Christchurch, New Zealand
P.H. Butler

National Centre for Physics, Quaid-I-Azam University, Islamabad, Pakistan
A. Ahmad, M. Ahmad, Q. Hassan, H.R. Hoorani, A. Saddique, M.A. Shah, M. Shoaib, M. Waqas

National Centre for Nuclear Research, Swierk, Poland
H. Bialkowska, M. Bluj, B. Boimska, T. Frueboes, M. Górski, M. Kazana, K. Nawrocki, M. Szleper, P. Traczyk, P. Zalewski

Institute of Experimental Physics, Faculty of Physics, University of Warsaw, Warsaw, Poland
K. Bunkowski, A. Byszuk[37], K. Doroba, A. Kalinowski, M. Konecki, J. Krolikowski, M. Misiura, M. Olszewski, A. Pyskir, M. Walczak

Laboratório de Instrumentação e Física Experimental de Partículas, Lisboa, Portugal
P. Bargassa, C. Beirão Da Cruz E Silva, A. Di Francesco, P. Faccioli, B. Galinhas, M. Gallinaro, J. Hollar, N. Leonardo, L. Lloret Iglesias, M.V. Nemallapudi, J. Seixas, G. Strong, O. Toldaiev, D. Vadruccio, J. Varela

Joint Institute for Nuclear Research, Dubna, Russia
S. Afanasiev, P. Bunin, M. Gavrilenko, I. Golutvin, I. Gorbunov, A. Kamenev, V. Karjavin, A. Lanev, A. Malakhov, V. Matveev[38,39], P. Moisenz, V. Palichik, V. Perelygin, S. Shmatov, S. Shulha, N. Skatchkov, V. Smirnov, N. Voytishin, A. Zarubin

Petersburg Nuclear Physics Institute, Gatchina (St. Petersburg), Russia
Y. Ivanov, V. Kim[40], E. Kuznetsova[41], P. Levchenko, V. Murzin, V. Oreshkin, I. Smirnov, D. Sosnov, V. Sulimov, L. Uvarov, S. Vavilov, A. Vorobyev

Institute for Nuclear Research, Moscow, Russia
Yu. Andreev, A. Dermenev, S. Gninenko, N. Golubev, A. Karneyeu, M. Kirsanov, N. Krasnikov, A. Pashenkov, D. Tlisov, A. Toropin

Institute for Theoretical and Experimental Physics, Moscow, Russia
V. Epshteyn, V. Gavrilov, N. Lychkovskaya, V. Popov, I. Pozdnyakov, G. Safronov, A. Spiridonov, A. Stepennov, V. Stolin, M. Toms, E. Vlasov, A. Zhokin

Moscow Institute of Physics and Technology, Moscow, Russia
T. Aushev, A. Bylinkin[39]

National Research Nuclear University 'Moscow Engineering Physics Institute' (MEPhI), Moscow, Russia
M. Chadeeva[42], R. Chistov[42], P. Parygin, D. Philippov, S. Polikarpov, E. Tarkovskii, E. Zhemchugov

P.N. Lebedev Physical Institute, Moscow, Russia
V. Andreev, M. Azarkin[39], I. Dremin[39], M. Kirakosyan[39], S.V. Rusakov, A. Terkulov

Skobeltsyn Institute of Nuclear Physics, Lomonosov Moscow State University, Moscow, Russia
A. Baskakov, A. Belyaev, E. Boos, M. Dubinin[43], L. Dudko, A. Ershov, A. Gribushin, V. Klyukhin, O. Kodolova, I. Lokhtin, I. Miagkov, S. Obraztsov, S. Petrushanko, V. Savrin, A. Snigirev

Novosibirsk State University (NSU), Novosibirsk, Russia
V. Blinov[44], D. Shtol[44], Y. Skovpen[44]

State Research Center of Russian Federation, Institute for High Energy Physics of NRC &quot, Kurchatov Institute&quot, , Protvino, Russia
I. Azhgirey, I. Bayshev, S. Bitioukov, D. Elumakhov, A. Godizov, V. Kachanov, A. Kalinin, D. Konstantinov, P. Mandrik, V. Petrov, R. Ryutin, A. Sobol, S. Troshin, N. Tyurin, A. Uzunian, A. Volkov

National Research Tomsk Polytechnic University, Tomsk, Russia
A. Babaev

University of Belgrade, Faculty of Physics and Vinca Institute of Nuclear Sciences, Belgrade, Serbia
P. Adzic[45], P. Cirkovic, D. Devetak, M. Dordevic, J. Milosevic

Centro de Investigaciones Energéticas Medioambientales y Tecnológicas (CIEMAT), Madrid, Spain
J. Alcaraz Maestre, A. Álvarez Fernández, I. Bachiller, M. Barrio Luna, M. Cerrada, N. Colino, B. De La Cruz, A. Delgado Peris, C. Fernandez Bedoya, J.P. Fernández Ramos, J. Flix, M.C. Fouz, O. Gonzalez Lopez, S. Goy Lopez, J.M. Hernandez, M.I. Josa, D. Moran, A. Pérez-Calero Yzquierdo, J. Puerta Pelayo, I. Redondo, L. Romero, M.S. Soares, A. Triossi

Universidad Autónoma de Madrid, Madrid, Spain
C. Albajar, J.F. de Trocóniz

Universidad de Oviedo, Oviedo, Spain
J. Cuevas, C. Erice, J. Fernandez Menendez, S. Folgueras, I. Gonzalez Caballero, J.R. González Fernández, E. Palencia Cortezon, S. Sanchez Cruz, P. Vischia, J.M. Vizan Garcia

Instituto de Física de Cantabria (IFCA), CSIC-Universidad de Cantabria, Santander, Spain
I.J. Cabrillo, A. Calderon, B. Chazin Quero, J. Duarte Campderros, M. Fernandez, P.J. Fernández Manteca, A. García Alonso, J. Garcia-Ferrero, G. Gomez, A. Lopez Virto, J. Marco, C. Martinez Rivero, P. Martinez Ruiz del Arbol, F. Matorras, J. Piedra Gomez, C. Prieels, T. Rodrigo, A. Ruiz-Jimeno, L. Scodellaro, N. Trevisani, I. Vila, R. Vilar Cortabitarte

CERN, European Organization for Nuclear Research, Geneva, Switzerland
D. Abbaneo, B. Akgun, E. Auffray, P. Baillon, A.H. Ball, D. Barney, J. Bendavid, M. Bianco, A. Bocci, C. Botta, T. Camporesi, M. Cepeda, G. Cerminara, E. Chapon, Y. Chen, D. d'Enterria, A. Dabrowski, V. Daponte, A. David, M. De Gruttola, A. De Roeck, N. Deelen, M. Dobson, T. du Pree, M. Dünser, N. Dupont, A. Elliott-Peisert, P. Everaerts, F. Fallavollita[46], G. Franzoni, J. Fulcher, W. Funk, D. Gigi, A. Gilbert, K. Gill, F. Glege, D. Gulhan, J. Hegeman, V. Innocente, A. Jafari, P. Janot, O. Karacheban[20], J. Kieseler, V. Knünz, A. Kornmayer, M. Krammer[1], C. Lange, P. Lecoq, C. Lourenço, M.T. Lucchini, L. Malgeri, M. Mannelli, A. Martelli, F. Meijers, J.A. Merlin, S. Mersi, E. Meschi, P. Milenovic[47], F. Moortgat, M. Mulders, H. Neugebauer, J. Ngadiuba, S. Orfanelli, L. Orsini, F. Pantaleo[17], L. Pape, E. Perez, M. Peruzzi, A. Petrilli, G. Petrucciani, A. Pfeiffer, M. Pierini, F.M. Pitters, D. Rabady, A. Racz, T. Reis, G. Rolandi[48], M. Rovere, H. Sakulin, C. Schäfer, C. Schwick, M. Seidel, M. Selvaggi, A. Sharma, P. Silva,

P. Sphicas[49], A. Stakia, J. Steggemann, M. Stoye, M. Tosi, D. Treille, A. Tsirou, V. Veckalns[50], M. Verweij, W.D. Zeuner

Paul Scherrer Institut, Villigen, Switzerland
W. Bertl[†], L. Caminada[51], K. Deiters, W. Erdmann, R. Horisberger, Q. Ingram, H.C. Kaestli, D. Kotlinski, U. Langenegger, T. Rohe, S.A. Wiederkehr

ETH Zurich - Institute for Particle Physics and Astrophysics (IPA), Zurich, Switzerland
M. Backhaus, L. Bäni, P. Berger, B. Casal, N. Chernyavskaya, G. Dissertori, M. Dittmar, M. Donegà, C. Dorfer, C. Grab, C. Heidegger, D. Hits, J. Hoss, T. Klijnsma, W. Lustermann, M. Marionneau, M.T. Meinhard, D. Meister, F. Micheli, P. Musella, F. Nessi-Tedaldi, J. Pata, F. Pauss, G. Perrin, L. Perrozzi, M. Quittnat, M. Reichmann, D. Ruini, D.A. Sanz Becerra, M. Schönenberger, L. Shchutska, V.R. Tavolaro, K. Theofilatos, M.L. Vesterbacka Olsson, R. Wallny, D.H. Zhu

Universität Zürich, Zurich, Switzerland
T.K. Aarrestad, C. Amsler[52], D. Brzhechko, M.F. Canelli, A. De Cosa, R. Del Burgo, S. Donato, C. Galloni, T. Hreus, B. Kilminster, I. Neutelings, D. Pinna, G. Rauco, P. Robmann, D. Salerno, K. Schweiger, C. Seitz, Y. Takahashi, A. Zucchetta

National Central University, Chung-Li, Taiwan
V. Candelise, Y.H. Chang, K.y. Cheng, T.H. Doan, Sh. Jain, R. Khurana, C.M. Kuo, W. Lin, A. Pozdnyakov, S.S. Yu

National Taiwan University (NTU), Taipei, Taiwan
P. Chang, Y. Chao, K.F. Chen, P.H. Chen, F. Fiori, W.-S. Hou, Y. Hsiung, Arun Kumar, Y.F. Liu, R.-S. Lu, E. Paganis, A. Psallidas, A. Steen, J.f. Tsai

Chulalongkorn University, Faculty of Science, Department of Physics, Bangkok, Thailand
B. Asavapibhop, K. Kovitanggoon, G. Singh, N. Srimanobhas

Çukurova University, Physics Department, Science and Art Faculty, Adana, Turkey
A. Bat, F. Boran, S. Cerci[53], S. Damarseckin, Z.S. Demiroglu, C. Dozen, I. Dumanoglu, S. Girgis, G. Gokbulut, Y. Guler, I. Hos[54], E.E. Kangal[55], O. Kara, A. Kayis Topaksu, U. Kiminsu, M. Oglakci, G. Onengut, K. Ozdemir[56], D. Sunar Cerci[53], B. Tali[53], U.G. Tok, S. Turkcapar, I.S. Zorbakir, C. Zorbilmez

Middle East Technical University, Physics Department, Ankara, Turkey
G. Karapinar[57], K. Ocalan[58], M. Yalvac, M. Zeyrek

Bogazici University, Istanbul, Turkey
E. Gülmez, M. Kaya[59], O. Kaya[60], S. Tekten, E.A. Yetkin[61]

Istanbul Technical University, Istanbul, Turkey
M.N. Agaras, S. Atay, A. Cakir, K. Cankocak, Y. Komurcu

Institute for Scintillation Materials of National Academy of Science of Ukraine, Kharkov, Ukraine
B. Grynyov

National Scientific Center, Kharkov Institute of Physics and Technology, Kharkov, Ukraine
L. Levchuk

University of Bristol, Bristol, United Kingdom
F. Ball, L. Beck, J.J. Brooke, D. Burns, E. Clement, D. Cussans, O. Davignon, H. Flacher,

J. Goldstein, G.P. Heath, H.F. Heath, L. Kreczko, D.M. Newbold[62], S. Paramesvaran, T. Sakuma, S. Seif El Nasr-storey, D. Smith, V.J. Smith

Rutherford Appleton Laboratory, Didcot, United Kingdom
K.W. Bell, A. Belyaev[63], C. Brew, R.M. Brown, D. Cieri, D.J.A. Cockerill, J.A. Coughlan, K. Harder, S. Harper, J. Linacre, E. Olaiya, D. Petyt, C.H. Shepherd-Themistocleous, A. Thea, I.R. Tomalin, T. Williams, W.J. Womersley

Imperial College, London, United Kingdom
G. Auzinger, R. Bainbridge, P. Bloch, J. Borg, S. Breeze, O. Buchmuller, A. Bundock, S. Casasso, D. Colling, L. Corpe, P. Dauncey, G. Davies, M. Della Negra, R. Di Maria, A. Elwood, Y. Haddad, G. Hall, G. Iles, T. James, M. Komm, R. Lane, C. Laner, L. Lyons, A.-M. Magnan, S. Malik, L. Mastrolorenzo, T. Matsushita, J. Nash[64], A. Nikitenko[7], V. Palladino, M. Pesaresi, A. Richards, A. Rose, E. Scott, C. Seez, A. Shtipliyski, T. Strebler, S. Summers, A. Tapper, K. Uchida, M. Vazquez Acosta[65], T. Virdee[17], N. Wardle, D. Winterbottom, J. Wright, S.C. Zenz

Brunel University, Uxbridge, United Kingdom
J.E. Cole, P.R. Hobson, A. Khan, P. Kyberd, A. Morton, I.D. Reid, L. Teodorescu, S. Zahid

Baylor University, Waco, USA
A. Borzou, K. Call, J. Dittmann, K. Hatakeyama, H. Liu, N. Pastika, C. Smith

Catholic University of America, Washington DC, USA
R. Bartek, A. Dominguez

The University of Alabama, Tuscaloosa, USA
A. Buccilli, S.I. Cooper, C. Henderson, P. Rumerio, C. West

Boston University, Boston, USA
D. Arcaro, A. Avetisyan, T. Bose, D. Gastler, D. Rankin, C. Richardson, J. Rohlf, L. Sulak, D. Zou

Brown University, Providence, USA
G. Benelli, D. Cutts, M. Hadley, J. Hakala, U. Heintz, J.M. Hogan[66], K.H.M. Kwok, E. Laird, G. Landsberg, J. Lee, Z. Mao, M. Narain, J. Pazzini, S. Piperov, S. Sagir, R. Syarif, D. Yu

University of California, Davis, Davis, USA
R. Band, C. Brainerd, R. Breedon, D. Burns, M. Calderon De La Barca Sanchez, M. Chertok, J. Conway, R. Conway, P.T. Cox, R. Erbacher, C. Flores, G. Funk, W. Ko, R. Lander, C. Mclean, M. Mulhearn, D. Pellett, J. Pilot, S. Shalhout, M. Shi, J. Smith, D. Stolp, D. Taylor, K. Tos, M. Tripathi, Z. Wang, F. Zhang

University of California, Los Angeles, USA
M. Bachtis, C. Bravo, R. Cousins, A. Dasgupta, A. Florent, J. Hauser, M. Ignatenko, N. Mccoll, S. Regnard, D. Saltzberg, C. Schnaible, V. Valuev

University of California, Riverside, Riverside, USA
E. Bouvier, K. Burt, R. Clare, J. Ellison, J.W. Gary, S.M.A. Ghiasi Shirazi, G. Hanson, G. Karapostoli, E. Kennedy, F. Lacroix, O.R. Long, M. Olmedo Negrete, M.I. Paneva, W. Si, L. Wang, H. Wei, S. Wimpenny, B. R. Yates

University of California, San Diego, La Jolla, USA
J.G. Branson, S. Cittolin, M. Derdzinski, R. Gerosa, D. Gilbert, B. Hashemi, A. Holzner, D. Klein, G. Kole, V. Krutelyov, J. Letts, M. Masciovecchio, D. Olivito, S. Padhi, M. Pieri, M. Sani, V. Sharma, S. Simon, M. Tadel, A. Vartak, S. Wasserbaech[67], J. Wood, F. Würthwein, A. Yagil, G. Zevi Della Porta

University of California, Santa Barbara - Department of Physics, Santa Barbara, USA
N. Amin, R. Bhandari, J. Bradmiller-Feld, C. Campagnari, M. Citron, A. Dishaw, V. Dutta, M. Franco Sevilla, L. Gouskos, R. Heller, J. Incandela, A. Ovcharova, H. Qu, J. Richman, D. Stuart, I. Suarez, J. Yoo

California Institute of Technology, Pasadena, USA
D. Anderson, A. Bornheim, J. Bunn, J.M. Lawhorn, H.B. Newman, T. Q. Nguyen, C. Pena, M. Spiropulu, J.R. Vlimant, R. Wilkinson, S. Xie, Z. Zhang, R.Y. Zhu

Carnegie Mellon University, Pittsburgh, USA
M.B. Andrews, T. Ferguson, T. Mudholkar, M. Paulini, J. Russ, M. Sun, H. Vogel, I. Vorobiev, M. Weinberg

University of Colorado Boulder, Boulder, USA
J.P. Cumalat, W.T. Ford, F. Jensen, A. Johnson, M. Krohn, S. Leontsinis, E. MacDonald, T. Mulholland, K. Stenson, K.A. Ulmer, S.R. Wagner

Cornell University, Ithaca, USA
J. Alexander, J. Chaves, Y. Cheng, J. Chu, A. Datta, K. Mcdermott, N. Mirman, J.R. Patterson, D. Quach, A. Rinkevicius, A. Ryd, L. Skinnari, L. Soffi, S.M. Tan, Z. Tao, J. Thom, J. Tucker, P. Wittich, M. Zientek

Fermi National Accelerator Laboratory, Batavia, USA
S. Abdullin, M. Albrow, M. Alyari, G. Apollinari, A. Apresyan, A. Apyan, S. Banerjee, L.A.T. Bauerdick, A. Beretvas, J. Berryhill, P.C. Bhat, G. Bolla[†], K. Burkett, J.N. Butler, A. Canepa, G.B. Cerati, H.W.K. Cheung, F. Chlebana, M. Cremonesi, J. Duarte, V.D. Elvira, J. Freeman, Z. Gecse, E. Gottschalk, L. Gray, D. Green, S. Grünendahl, O. Gutsche, J. Hanlon, R.M. Harris, S. Hasegawa, J. Hirschauer, Z. Hu, B. Jayatilaka, S. Jindariani, M. Johnson, U. Joshi, B. Klima, M.J. Kortelainen, B. Kreis, S. Lammel, D. Lincoln, R. Lipton, M. Liu, T. Liu, R. Lopes De Sá, J. Lykken, K. Maeshima, N. Magini, J.M. Marraffino, D. Mason, P. McBride, P. Merkel, S. Mrenna, S. Nahn, V. O'Dell, K. Pedro, O. Prokofyev, G. Rakness, L. Ristori, A. Savoy-Navarro[68], B. Schneider, E. Sexton-Kennedy, A. Soha, W.J. Spalding, L. Spiegel, S. Stoynev, J. Strait, N. Strobbe, L. Taylor, S. Tkaczyk, N.V. Tran, L. Uplegger, E.W. Vaandering, C. Vernieri, M. Verzocchi, R. Vidal, M. Wang, H.A. Weber, A. Whitbeck, W. Wu

University of Florida, Gainesville, USA
D. Acosta, P. Avery, P. Bortignon, D. Bourilkov, A. Brinkerhoff, A. Carnes, M. Carver, D. Curry, R.D. Field, I.K. Furic, S.V. Gleyzer, B.M. Joshi, J. Konigsberg, A. Korytov, K. Kotov, P. Ma, K. Matchev, H. Mei, G. Mitselmakher, K. Shi, D. Sperka, N. Terentyev, L. Thomas, J. Wang, S. Wang, J. Yelton

Florida International University, Miami, USA
Y.R. Joshi, S. Linn, P. Markowitz, J.L. Rodriguez

Florida State University, Tallahassee, USA
A. Ackert, T. Adams, A. Askew, S. Hagopian, V. Hagopian, K.F. Johnson, T. Kolberg, G. Martinez, T. Perry, H. Prosper, A. Saha, A. Santra, V. Sharma, R. Yohay

Florida Institute of Technology, Melbourne, USA
M.M. Baarmand, V. Bhopatkar, S. Colafranceschi, M. Hohlmann, D. Noonan, T. Roy, F. Yumiceva

University of Illinois at Chicago (UIC), Chicago, USA
M.R. Adams, L. Apanasevich, D. Berry, R.R. Betts, R. Cavanaugh, X. Chen, S. Dittmer, O. Ev-

dokimov, C.E. Gerber, D.A. Hangal, D.J. Hofman, K. Jung, J. Kamin, I.D. Sandoval Gonzalez, M.B. Tonjes, N. Varelas, H. Wang, Z. Wu, J. Zhang

The University of Iowa, Iowa City, USA
B. Bilki[69], W. Clarida, K. Dilsiz[70], S. Durgut, R.P. Gandrajula, M. Haytmyradov, V. Khristenko, J.-P. Merlo, H. Mermerkaya[71], A. Mestvirishvili, A. Moeller, J. Nachtman, H. Ogul[72], Y. Onel, F. Ozok[73], A. Penzo, C. Snyder, E. Tiras, J. Wetzel, K. Yi

Johns Hopkins University, Baltimore, USA
B. Blumenfeld, A. Cocoros, N. Eminizer, D. Fehling, L. Feng, A.V. Gritsan, W.T. Hung, P. Maksimovic, J. Roskes, U. Sarica, M. Swartz, M. Xiao, C. You

The University of Kansas, Lawrence, USA
A. Al-bataineh, P. Baringer, A. Bean, S. Boren, J. Bowen, J. Castle, L. Forthomme, S. Khalil, A. Kropivnitskaya, D. Majumder, W. Mcbrayer, M. Murray, C. Rogan, C. Royon, S. Sanders, E. Schmitz, J.D. Tapia Takaki, Q. Wang

Kansas State University, Manhattan, USA
A. Ivanov, K. Kaadze, Y. Maravin, A. Modak, A. Mohammadi, L.K. Saini, N. Skhirtladze

Lawrence Livermore National Laboratory, Livermore, USA
F. Rebassoo, D. Wright

University of Maryland, College Park, USA
A. Baden, O. Baron, A. Belloni, S.C. Eno, Y. Feng, C. Ferraioli, N.J. Hadley, S. Jabeen, G.Y. Jeng, R.G. Kellogg, J. Kunkle, A.C. Mignerey, F. Ricci-Tam, Y.H. Shin, A. Skuja, S.C. Tonwar

Massachusetts Institute of Technology, Cambridge, USA
D. Abercrombie, B. Allen, V. Azzolini, R. Barbieri, A. Baty, G. Bauer, R. Bi, S. Brandt, W. Busza, I.A. Cali, M. D'Alfonso, Z. Demiragli, G. Gomez Ceballos, M. Goncharov, P. Harris, D. Hsu, M. Hu, Y. Iiyama, G.M. Innocenti, M. Klute, D. Kovalskyi, Y.-J. Lee, A. Levin, P.D. Luckey, B. Maier, A.C. Marini, C. Mcginn, C. Mironov, S. Narayanan, X. Niu, C. Paus, C. Roland, G. Roland, G.S.F. Stephans, K. Sumorok, K. Tatar, D. Velicanu, J. Wang, T.W. Wang, B. Wyslouch, S. Zhaozhong

University of Minnesota, Minneapolis, USA
A.C. Benvenuti, R.M. Chatterjee, A. Evans, P. Hansen, S. Kalafut, Y. Kubota, Z. Lesko, J. Mans, S. Nourbakhsh, N. Ruckstuhl, R. Rusack, J. Turkewitz, M.A. Wadud

University of Mississippi, Oxford, USA
J.G. Acosta, S. Oliveros

University of Nebraska-Lincoln, Lincoln, USA
E. Avdeeva, K. Bloom, D.R. Claes, C. Fangmeier, F. Golf, R. Gonzalez Suarez, R. Kamalieddin, I. Kravchenko, J. Monroy, J.E. Siado, G.R. Snow, B. Stieger

State University of New York at Buffalo, Buffalo, USA
A. Godshalk, C. Harrington, I. Iashvili, D. Nguyen, A. Parker, S. Rappoccio, B. Roozbahani

Northeastern University, Boston, USA
G. Alverson, E. Barberis, C. Freer, A. Hortiangtham, A. Massironi, D.M. Morse, T. Orimoto, R. Teixeira De Lima, T. Wamorkar, B. Wang, A. Wisecarver, D. Wood

Northwestern University, Evanston, USA
S. Bhattacharya, O. Charaf, K.A. Hahn, N. Mucia, N. Odell, M.H. Schmitt, K. Sung, M. Trovato, M. Velasco

University of Notre Dame, Notre Dame, USA
R. Bucci, N. Dev, M. Hildreth, K. Hurtado Anampa, C. Jessop, D.J. Karmgard, N. Kellams, K. Lannon, W. Li, N. Loukas, N. Marinelli, F. Meng, C. Mueller, Y. Musienko[38], M. Planer, A. Reinsvold, R. Ruchti, P. Siddireddy, G. Smith, S. Taroni, M. Wayne, A. Wightman, M. Wolf, A. Woodard

The Ohio State University, Columbus, USA
J. Alimena, L. Antonelli, B. Bylsma, L.S. Durkin, S. Flowers, B. Francis, A. Hart, C. Hill, W. Ji, T.Y. Ling, W. Luo, B.L. Winer, H.W. Wulsin

Princeton University, Princeton, USA
S. Cooperstein, O. Driga, P. Elmer, J. Hardenbrook, P. Hebda, S. Higginbotham, A. Kalogeropoulos, D. Lange, J. Luo, D. Marlow, K. Mei, I. Ojalvo, J. Olsen, C. Palmer, P. Piroué, J. Salfeld-Nebgen, D. Stickland, C. Tully

University of Puerto Rico, Mayaguez, USA
S. Malik, S. Norberg

Purdue University, West Lafayette, USA
A. Barker, V.E. Barnes, S. Das, L. Gutay, M. Jones, A.W. Jung, A. Khatiwada, D.H. Miller, N. Neumeister, C.C. Peng, H. Qiu, J.F. Schulte, J. Sun, F. Wang, R. Xiao, W. Xie

Purdue University Northwest, Hammond, USA
T. Cheng, J. Dolen, N. Parashar

Rice University, Houston, USA
Z. Chen, K.M. Ecklund, S. Freed, F.J.M. Geurts, M. Guilbaud, M. Kilpatrick, W. Li, B. Michlin, B.P. Padley, J. Roberts, J. Rorie, W. Shi, Z. Tu, J. Zabel, A. Zhang

University of Rochester, Rochester, USA
A. Bodek, P. de Barbaro, R. Demina, Y.t. Duh, T. Ferbel, M. Galanti, A. Garcia-Bellido, J. Han, O. Hindrichs, A. Khukhunaishvili, K.H. Lo, P. Tan, M. Verzetti

The Rockefeller University, New York, USA
R. Ciesielski, K. Goulianos, C. Mesropian

Rutgers, The State University of New Jersey, Piscataway, USA
A. Agapitos, J.P. Chou, Y. Gershtein, T.A. Gómez Espinosa, E. Halkiadakis, M. Heindl, E. Hughes, S. Kaplan, R. Kunnawalkam Elayavalli, S. Kyriacou, A. Lath, R. Montalvo, K. Nash, M. Osherson, H. Saka, S. Salur, S. Schnetzer, D. Sheffield, S. Somalwar, R. Stone, S. Thomas, P. Thomassen, M. Walker

University of Tennessee, Knoxville, USA
A.G. Delannoy, J. Heideman, G. Riley, K. Rose, S. Spanier, K. Thapa

Texas A&M University, College Station, USA
O. Bouhali[74], A. Castaneda Hernandez[74], A. Celik, M. Dalchenko, M. De Mattia, A. Delgado, S. Dildick, R. Eusebi, J. Gilmore, T. Huang, T. Kamon[75], R. Mueller, Y. Pakhotin, R. Patel, A. Perloff, L. Perniè, D. Rathjens, A. Safonov, A. Tatarinov

Texas Tech University, Lubbock, USA
N. Akchurin, J. Damgov, F. De Guio, P.R. Dudero, J. Faulkner, E. Gurpinar, S. Kunori, K. Lamichhane, S.W. Lee, T. Mengke, S. Muthumuni, T. Peltola, S. Undleeb, I. Volobouev, Z. Wang

Vanderbilt University, Nashville, USA
S. Greene, A. Gurrola, R. Janjam, W. Johns, C. Maguire, A. Melo, H. Ni, K. Padeken, J.D. Ruiz Alvarez, P. Sheldon, S. Tuo, J. Velkovska, Q. Xu

University of Virginia, Charlottesville, USA
M.W. Arenton, P. Barria, B. Cox, R. Hirosky, M. Joyce, A. Ledovskoy, H. Li, C. Neu, T. Sinthuprasith, Y. Wang, E. Wolfe, F. Xia

Wayne State University, Detroit, USA
R. Harr, P.E. Karchin, N. Poudyal, J. Sturdy, P. Thapa, S. Zaleski

University of Wisconsin - Madison, Madison, WI, USA
M. Brodski, J. Buchanan, C. Caillol, D. Carlsmith, S. Dasu, L. Dodd, S. Duric, B. Gomber, M. Grothe, M. Herndon, A. Hervé, U. Hussain, P. Klabbers, A. Lanaro, A. Levine, K. Long, R. Loveless, V. Rekovic, T. Ruggles, A. Savin, N. Smith, W.H. Smith, N. Woods

†: Deceased
1: Also at Vienna University of Technology, Vienna, Austria
2: Also at IRFU; CEA; Université Paris-Saclay, Gif-sur-Yvette, France
3: Also at Universidade Estadual de Campinas, Campinas, Brazil
4: Also at Federal University of Rio Grande do Sul, Porto Alegre, Brazil
5: Also at Universidade Federal de Pelotas, Pelotas, Brazil
6: Also at Université Libre de Bruxelles, Bruxelles, Belgium
7: Also at Institute for Theoretical and Experimental Physics, Moscow, Russia
8: Also at Joint Institute for Nuclear Research, Dubna, Russia
9: Now at Cairo University, Cairo, Egypt
10: Also at Zewail City of Science and Technology, Zewail, Egypt
11: Also at British University in Egypt, Cairo, Egypt
12: Now at Ain Shams University, Cairo, Egypt
13: Also at Department of Physics; King Abdulaziz University, Jeddah, Saudi Arabia
14: Also at Université de Haute Alsace, Mulhouse, France
15: Also at Skobeltsyn Institute of Nuclear Physics; Lomonosov Moscow State University, Moscow, Russia
16: Also at Tbilisi State University, Tbilisi, Georgia
17: Also at CERN; European Organization for Nuclear Research, Geneva, Switzerland
18: Also at RWTH Aachen University; III. Physikalisches Institut A, Aachen, Germany
19: Also at University of Hamburg, Hamburg, Germany
20: Also at Brandenburg University of Technology, Cottbus, Germany
21: Also at MTA-ELTE Lendület CMS Particle and Nuclear Physics Group; Eötvös Loránd University, Budapest, Hungary
22: Also at Institute of Nuclear Research ATOMKI, Debrecen, Hungary
23: Also at Institute of Physics; University of Debrecen, Debrecen, Hungary
24: Also at Indian Institute of Technology Bhubaneswar, Bhubaneswar, India
25: Also at Institute of Physics, Bhubaneswar, India
26: Also at Shoolini University, Solan, India
27: Also at University of Visva-Bharati, Santiniketan, India
28: Also at University of Ruhuna, Matara, Sri Lanka
29: Also at Isfahan University of Technology, Isfahan, Iran
30: Also at Yazd University, Yazd, Iran
31: Also at Plasma Physics Research Center; Science and Research Branch; Islamic Azad University, Tehran, Iran

32: Also at Università degli Studi di Siena, Siena, Italy

33: Also at INFN Sezione di Milano-Bicocca; Università di Milano-Bicocca, Milano, Italy

34: Also at International Islamic University of Malaysia, Kuala Lumpur, Malaysia

35: Also at Malaysian Nuclear Agency; MOSTI, Kajang, Malaysia

36: Also at Consejo Nacional de Ciencia y Tecnología, Mexico city, Mexico

37: Also at Warsaw University of Technology; Institute of Electronic Systems, Warsaw, Poland

38: Also at Institute for Nuclear Research, Moscow, Russia

39: Now at National Research Nuclear University 'Moscow Engineering Physics Institute' (MEPhI), Moscow, Russia

40: Also at St. Petersburg State Polytechnical University, St. Petersburg, Russia

41: Also at University of Florida, Gainesville, USA

42: Also at P.N. Lebedev Physical Institute, Moscow, Russia

43: Also at California Institute of Technology, Pasadena, USA

44: Also at Budker Institute of Nuclear Physics, Novosibirsk, Russia

45: Also at Faculty of Physics; University of Belgrade, Belgrade, Serbia

46: Also at INFN Sezione di Pavia; Università di Pavia, Pavia, Italy

47: Also at University of Belgrade; Faculty of Physics and Vinca Institute of Nuclear Sciences, Belgrade, Serbia

48: Also at Scuola Normale e Sezione dell'INFN, Pisa, Italy

49: Also at National and Kapodistrian University of Athens, Athens, Greece

50: Also at Riga Technical University, Riga, Latvia

51: Also at Universität Zürich, Zurich, Switzerland

52: Also at Stefan Meyer Institute for Subatomic Physics (SMI), Vienna, Austria

53: Also at Adiyaman University, Adiyaman, Turkey

54: Also at Istanbul Aydin University, Istanbul, Turkey

55: Also at Mersin University, Mersin, Turkey

56: Also at Piri Reis University, Istanbul, Turkey

57: Also at Izmir Institute of Technology, Izmir, Turkey

58: Also at Necmettin Erbakan University, Konya, Turkey

59: Also at Marmara University, Istanbul, Turkey

60: Also at Kafkas University, Kars, Turkey

61: Also at Istanbul Bilgi University, Istanbul, Turkey

62: Also at Rutherford Appleton Laboratory, Didcot, United Kingdom

63: Also at School of Physics and Astronomy; University of Southampton, Southampton, United Kingdom

64: Also at Monash University; Faculty of Science, Clayton, Australia

65: Also at Instituto de Astrofísica de Canarias, La Laguna, Spain

66: Also at Bethel University, ST. PAUL, USA

67: Also at Utah Valley University, Orem, USA

68: Also at Purdue University, West Lafayette, USA

69: Also at Beykent University, Istanbul, Turkey

70: Also at Bingol University, Bingol, Turkey

71: Also at Erzincan University, Erzincan, Turkey

72: Also at Sinop University, Sinop, Turkey

73: Also at Mimar Sinan University; Istanbul, Istanbul, Turkey

74: Also at Texas A&M University at Qatar, Doha, Qatar

75: Also at Kyungpook National University, Daegu, Korea

B The TOTEM Collaboration

G. Antchev[a], P. Aspell[9], I. Atanassov[a], V. Avati[7,9], J. Baechler[9], C. Baldenegro Barrera[11], V. Berardi[4a,4b], M. Berretti[2a], E. Bossini[9,6b], U. Bottigli[6b], M. Bozzo[5a,5b], F. S. Cafagna[4a], M. G. Catanesi[4a], M. Csanád[3a,b], T. Csörgő[3a,3b], M. Deile[9], F. De Leonardis[4c,4a], A. D'Orazio[4c,4a], M. Doubek[1c], D. Druzhkin[9], K. Eggert[10], V. Eremin[e], A. Fiergolski[9], F. Garcia[2a], V. Georgiev[1a], S. Giani[9], L. Grzanka[7,c], J. Hammerbauer[1a], J. Heino[2a], T. Isidori[11], V. Ivanchenko[8], M. Janda[1c], A. Karev[9], J. Kašpar[6a,1b], J. Kopal[9], V. Kundrát[1b], S. Lami[6a], G. Latino[6b], R. Lauhakangas[2a], R. Linhart[1a], C. Lindsey[11], M. V. Lokajíček[1b], L. Losurdo[6b], M. Lo Vetere[5b,5a,†], F. Lucas Rodríguez[9], M. Macrí[5a], M. Malawski[7,c], N. Minafra[11], S. Minutoli[5a], T. Naaranoja[2a,2b], F. Nemes[9,3a], H. Niewiadomski[10], T. Novák[3b], E. Oliveri[9], F. Oljemark[2a,2b], M. Oriunno[f], K. Österberg[2a,2b], P. Palazzi[9], V. Passaro[4c,4a], Z. Peroutka[1a], J. Procházka[1b], M. Quinto[4a,4b], E. Radermacher[9], E. Radicioni[4a], F. Ravotti[9], G. Ruggiero[9], H. Saarikko[2a,2b], A. Scribano[6a], J. Siroky[1a], J. Smajek[9], W. Snoeys[9], R. Stefanovitch[9], J. Sziklai[3a], C. Taylor[10], E. Tcherniaev[8], N. Turini[6b], V. Vacek[1c], J. Welti[2a,2b], J. Williams[11], P. Wyszkowski[7], J. Zich[1a], K. Zielinski[7]

[1a]University of West Bohemia, Pilsen, Czech Republic.
[1b]Institute of Physics of the Academy of Sciences of the Czech Republic, Prague, Czech Republic.
[1c]Czech Technical University, Prague, Czech Republic.
[2a]Helsinki Institute of Physics, University of Helsinki, Helsinki, Finland.
[2b]Department of Physics, University of Helsinki, Helsinki, Finland.
[3a]Wigner Research Centre for Physics, RMKI, Budapest, Hungary.
[3b]EKU KRC, Gyöngyös, Hungary.
[4a]INFN Sezione di Bari, Bari, Italy.
[4b]Dipartimento Interateneo di Fisica di Bari, Bari, Italy.
[4c]Dipartimento di Ingegneria Elettrica e dell'Informazione — Politecnico di Bari, Bari, Italy.
[5a]INFN Sezione di Genova, Genova, Italy.
[5b]Università degli Studi di Genova, Italy.
[6a]INFN Sezione di Pisa, Pisa, Italy.
[6b]Università degli Studi di Siena and Gruppo Collegato INFN di Siena, Siena, Italy.
[7]AGH University of Science and Technology, Krakow, Poland.
[8]Tomsk State University, Tomsk, Russia.
[9]CERN, Geneva, Switzerland.
[10]Case Western Reserve University, Dept. of Physics, Cleveland, OH, USA.
[11]The University of Kansas, Lawrence, USA.

[a] INRNE-BAS, Institute for Nuclear Research and Nuclear Energy, Bulgarian Academy of Sciences, Sofia, Bulgaria.
[b] Department of Atomic Physics, ELTE University, Budapest, Hungary.
[c] Institute of Nuclear Physics, Polish Academy of Science, Krakow, Poland.
[d] Warsaw University of Technology, Warsaw, Poland.
[e] Ioffe Physical - Technical Institute of Russian Academy of Sciences, St. Petersburg, Russian Federation.
[f] SLAC National Accelerator Laboratory, Stanford CA, USA.
[†] Deceased.